THE ACCURACY OF STEREOPHOTOGRAMMETRY FOR COMPLETE-ARCH DIGITAL IMPLANT IMPRESSION IN VITRO AND IN VIVO

PhD Thesis

by

DR. ALESSANDRO POZZI, DDS

UNIVERSITY OF SZEGED, DOCTORAL SCHOOL OF CLINICAL MEDICINE

SUPERVISOR: PROF. KATALIN NAGY, DDS, PhD, DSc
UNIVERSITY OF SZEGED, FACULTY OF DENTISTRY, DEPARTMENT OF ORAL SURGERY

University of Szeged, Hungary

2023

TABLE OF CONTENTS

LIST OF PUBLICATIONS PROVIDING THE BASIS OF THE THESIS

1. **Pozzi A**, Agliardi E, Lio F, Nagy K, Nardi A, Arcuri L. Accuracy of intraoral optical scan versus stereophotogrammetry for complete-arch digital implant impression: An *in vitro* study. *J Prosthod Res.* 2023 Aug 11. doi: 10.2186/jpr.JPR_D_22_00251. Epub ahead of print.

Impact factor: 3.6

SJR rank: Q1

2. **Pozzi A**, Carosi P, Gallucci GO, Nagy K, Nardi A, Arcuri L. Accuracy of complete-arch digital implant impression with intraoral optical scanning and stereophotogrammetry: An in vivo prospective comparative study. *Clin Oral Implants Res*. 2023 Jul 24. doi: 10.1111/clr.14141. Epub ahead of print.

Impact factor: 4.3

SJR rank: Q1/D1

Summed impact factor: 7.9

ABBREVIATIONS

ASA	American Society of Anaesthesiologists
CAD-CAM	Computer-Assisted Design and Computer-Assisted Manufacturing
CBCT	Cone-Beam Computed Tomography
CCD	Charged Couple Device camera
CMM	coordinate measuring machine
DICOM	Digital imaging and communications in medicine (also .dcm, imaging file type)
FDP	fixed dental prosthesis
GCP	Good Clinical Practice (standardized way of conducting clinical trials as described in the international standard ISO 14155)
IOS	intraoral scanner
ISB	intraoral scan body
ISO	International Organization for Standardization
ISRCTN	International Standard Randomised Controlled Trial Number
ISQ	Implant Stability Quotient (Osstell)
ISZ-FDP	implant-supported, screw-retained zirconia complete-arch fixed dental prosthesis
PMMA	polymethyl methacrylate
RMS	root mean square
SD	standard deviation
SPG	stereophotogrammetry
SPG ISB	intraoral scan body for the purposes of stereophotogrammetry
STL	standard tessellation language (also .stl, stereolithography file type)

I. INTRODUCTION

I.1. General introductory remarks

Achieving long-term successful outcomes for screw-retained complete arch fixed dental prostheses (FDPs) relies on ensuring accurate matching between implants and frameworks [1]. The primary objective is to deliver an FDP that exhibits proper fit with the prosthetic platforms, minimizing the occurrence of mechanical complications [2, 3]. It is strongly recommended to achieve a passive fit with an accuracy of up to 150 micrometers [4-6]. In addition, a misfit between the prosthesis and implants may result in bacterial leakage and give rise to biological complications [7-9]. Therefore, precise recording of implant coordinates and accurate prosthetic manufacturing are essential prerequisites [6, 10].

The conventional approach for capturing implant impressions in complete arch cases is still widely regarded as the preferred method in complete-arch cases [11-13]. However, this workflow involves multiple steps, which does not only make it time-consuming, but also carries the risk of the cumulation of error [11, 14]. Furthermore, the subsequent requirement to digitize the master cast for CAD-CAM further complicates the overall process [15]. Finally, patients often find the conventional approach unpleasant, which obviously encourages the use of digital methods for impression taking [16, 17].

Intraoral optical surface scanning (IOS) systems have emerged and become widespread as the digital alternative to conventional impressions for capturing intraoral anatomy for various purposes, including the capturing of implant positions [18-23]. This innovative technique relies on sophisticated optical instruments, including high-resolution cameras and laser systems, to capture intricate 3D images of oral structures with remarkable accuracy [24-28]. Departing from conventional methods that involved physical impressions, intraoral optical scanning offers a contactless and more comfortable experience for patients, sidestepping the discomfort and inconvenience associated with impression materials [29-34]. Efficiency is another hallmark of intraoral optical scanning, influencing workflow dynamics in dental practices. The rapid capture of images, absence of material-setting time, and seamless integration with computer-aided design and manufacturing (CAD/CAM) systems collectively contribute to expedited procedures. This efficiency translates into reduced chair time for patients and quicker turnaround for restorations [35-37]. However, while the accuracy of IOS implant impressions has been established for single and short-span fixed dental prostheses (FDPs) [38], its application for complete arch implant impressions remains controversial, particularly for the lower jaw [2, 39]. The accuracy of intraoral scanning is influenced by various factors, including those related to the operator (such as scanning

technology and system selection, scanning head size, calibration, scanning distance, exposure of the IOS to ambient temperature changes, ambient humidity, ambient lighting conditions, operator experience, scanning pattern, extension of the scan, cutting off, rescanning, and overlapping) and patient factors (including tooth type, presence of interdental spaces, variations in arch width, palate characteristics, wetness, existing restorations, characteristics of the surface being digitized, edentulous areas, interimplant distance, position, angulation, and depth of existing implants, and the type of the applied implant scan bodies) [40, 41]. The main limitation of current IOS systems lies in their three-dimensional (3D) image reconstruction technology, which utilizes a best fit algorithm stitching process [12, 42-44]. To enhance the accuracy of consecutive 3D images, continuous reference points are essential to expedite the stitching process and improve matching accuracy [5, 26]. Various artificial landmark techniques have been proposed and tested positively in terms of accuracy, although they may introduce deviations and pose practical challenges [5, 45, 46]. All in all, while this technology has its undeniable advantages, it also still has its challenges, especially in the area of complete arch impressions.

Stereophotogrammetry (SPG) is a distinct digital impression technology that captures three-dimensional objects and their spatial relationship using points within photographic images from two stereo cameras [47]. Initially proposed by Lie and Jemt as a method to measure the misfit between implants and frameworks [48], SPG has been established as a reliable technology for digitally planned, dynamically guided implant treatment as it utilizes a stereo tracking algorithm that can connect preoperative implant planning coordinates with live-tracked drilling and positioning coordinates [49]. SPG allows the recording of the implant coordinates without the need for stitching, like in the case of IOSs. However, it cannot capture intraoral dental and gingival anatomy, which necessitates integration with an auxiliary impression [50]. A further relative drawback is that the global market currently offers a limited number of SPG devices, and their cost surpasses that of IOS systems. The first randomized, controlled clinical trial to establish if SPG might be suitable for digital impression taking for FDPs was published in 2017 by Peñarrocha-Diago and co-workers and concluded that digital impressions using stereophotogrammetry may be an alternative to traditional impressions [51].

I.2. Stereophotogrammetry for digital impression taking

In general, SPG is a technique used to capture and measure three-dimensional (3D) objects and their spatial relationships using stereo cameras. It involves taking multiple photographs of an object or scene from different angles and using the information from these images to reconstruct

the 3D structure of the object. By analyzing the differences in perspective between the two camera views, stereophotogrammetry can accurately determine the position, size, and shape of objects in 3D space. SPG is used in various areas of medicine [52-55].

SPG, as a digital impression technique, rests on two key elements: a stereocamera (Fig.1) and special stereophotogrammetry abutments (Fig.2). The essence of the technique is the digital determination of implant positions based on the principle that if the position one element (the special abutment) is known in the space, then the position of another element attached to it (the implant) can be exactly calculated, provided that the dimensions of the latter are known.

Regarding the clinical procedure, the camera is located 15 to 30 cm from the patient's mouth at an angle of no more than 45° to the abutments. The camera then takes 50-60 3D images of each abutment pair. The error margin is under 10 μm [6, 56]. The camera has a built-in infrared flash that eliminates shadows cast by ambient light [50]. During the capture, all abutments must be visible to the camera. If it is not possible (for instance, when 5 or more implants are scanned), the procedure should be done in two phases.

A great clinical advantage of this approach is that the presence of organic or inorganic residues on the surfaces does not affect either the success of the procedure or its accuracy [50].

Fig.1: A PIC SPG camera (PIC Dental, Spain) in use. The unit is attached to a mobile computer station where image processing happens. Image courtesy of PIC Dental.

Fig.2: The special SPG abutments (PIC abutments, PIC Dental, Spain) screwed onto implants in a patient's mouth. Image courtesy of PIC Dental.

On the other hand, as briefly mentioned previously, SPG does not register the peri-implant soft tissues. The output is a file (PIC file) that contains the vectorial relationship between the implant prosthetic platforms. To allow actual prosthetic planning, this needs to be registered with the image of the soft tissues. To reach that end, one must obtain an image of the soft tissues. For this, healing abutments are screwed on each implant. At this point, care must be taken that the abutments are of the same height, so that the software can exactly determine the depth of the implant platform. Once the healing abutments are in place, one can either utilize an IOS to get an image of the soft tissues or fabricate a type IV stone cast (a master model) that is then scanned with an extraoral scanner. Either way, the goal is to get an .stl file that can be registered with the PIC file in a software fit for this purpose (such as Exocad). This is naturally followed by several technical steps, such as checking the occlusal relations with the help of an antagonist scan, but for the purposes of this brief introduction, I will refrain from discussing these in detail, as they are only loosely relevant to the subject of this thesis. The interested reader can find details in the works of Agustín-Panadero and co-workers [50, 51, 56].

In vitro studies analyzed SPG accuracy for complete arch implant impressions reporting controversial results [39, 57, 58], and so far we know of only a pilot clinical trial that tested SPG for such purposes [51]. While the overall picture is promising, we have too little evidence on the accuracy of SPG for complete arch implant impressions. This is why our research group decided to examine this question both *in vitro* and *in vivo*, in comparison to the most widespread digital impression technology: IOS. The comparison was logical not only because both approaches are

digital, but also because SPG promises to overcome the shortcomings of IOS for this specific indication.

For the purposes of this thesis and the studies it is based on, the definitions of ISO 5725-1:1994 (Accuracy (trueness and precision) of measurement methods and results - Part 1: General principles and definitions) were used. According to the standard, accuracy is defined by trueness and precision; trueness describes the conformity of measurements to the actual values, and precision describes the conformity of multiple repeated measurements.

II. OBJECTIVES AND HYPOTHESES

In this thesis, two studies are covered. Both dealt with the accuracy of SPG for complete arch implant impressions, and whether SPG is in fact superior to IOS in this indication.

The first study (Pozzi et al., 2023, *JProsthodRes*) examined these questions *in vitro*. The purpose was to assess and compare accuracy of an intraoral scanner (IOS) and a stereophotogrammetry (SPG) device for complete-arch digital implant impressions. A 4-analog model was digitized with a desk scanner to achieve a reference file. Thirty test scans were recorded with an IOS and further 30 with an SPG device. The scans were then aligned to the reference file to calculate deviations. The null hypothesis was that no significant difference would be found in the 3D and angular deviations between the investigated complete-arch digital implant impression techniques.

The second study (Pozzi et al., 2023, *Clin Oral Implants Res*) examined the same questions *in vivo*, in a clinical population. The study recruited patients who required implant-supported screw-retained zirconia complete-arch fixed dental prostheses (ISZ-FDP). For each patient, both IOS and SPG scans (test impressions), and open-tray plaster impressions (reference) were taken. A total of 50 implants (100 images) were captured by the 2 investigated devices and compared to the reference. The study examined the same parameters of deviation as the *in vitro* study. The null hypothesis was that SPG and IOS would show similar accuracy, without significant difference between the devices.

III. METHODS

III. 1. Methods of the *in vitro* study

III.1.1. The master model and the reference scan

A milled edentulous mandible model made of polymethylmetacrylate (PMMA) was created, featuring four multiunit implant analogs (MUA, NobelBiocare, Switzerland). These analogs were positioned at the specific locations of teeth 32, 35, 42, and 45. The implant positioning followed the following criteria: tooth 32 (with a depth offset of -1 mm and a distal angulation of 5°), tooth 35 (with a depth offset of -3 mm and a mesial angulation of 10°), tooth 42 (at a depth of 0 mm and an angulation of 0°), and tooth 45 (with a depth offset of -4 mm and a distal angulation of 15°). To ensure the accurate fit of scanbodies (ISBs) on the model and to allow for fit verification, a removable soft tissue frame was 3D printed using specialized material (Gingiva Mask, NextDent) on a NextDent 5100 printer from 3D Systems in the USA, based in Rock Hill, SC.

To generate the reference scan, a D2000 dental laboratory scanner (3Shape, Copenhagen, Denmark), which had undergone meticulous calibration before the scanning process, was employed. The purpose was to obtain an .stl file that would serve as the designated reference. This scanner holds certification attesting to its accuracy level of 5 μm.

III.1.2. Intraoral scanning and stereophotogrammetry

An experienced operator, who remained unaware of the study's objectives, was enlisted for both scanning instruments. Another operator was responsible for affixing the polyether ether ketone (PEEK) ISBs onto the MUA implant analogs (Fig.3 top). This attachment was achieved using a dynamometer-controlled torque of 10 Ncm. To ensure proper seating of the ISBs over the analog heads, visual verification was performed with magnifying loupes (Eyezoom 5X, Orascoptic, located in Middleton, WI, USA). Following this step, the same operator proceeded to affix SPG scanbodies onto the MUA implant analogs using an identical procedure (Fig. 3 bottom). The process culminated in a total of 60 comprehensive arch scans, with 30 scans executed for each of the two scanning devices.

For the intraoral scans, we used iTero Element 5D (Align Technology, Tempe, AZ, USA). This is a pen-grip style scanner, which operates without the need for powder and functions through parallel confocal imaging laser technology. During the IOS scanning process, each scan was separated by a rest interval of at least 5 minutes. Commencing at ISB position 45 and concluding with 35, the scan sequence was consistently maintained. Before initiating the investigation, calibration of the IOS device was executed by the manufacturer.

The scan strategy remained uniform across all scanning procedures, adhering to the recommendations provided by the manufacturer. The scanning process commenced from the occlusal-lingual surface of ISB 45, progressed to include both surfaces of each ISB, and concluded by returning from the buccal side [59].

Fig.3: Top: mandibular PMMA model with removable soft tissue frame and PEEK ISBs screwed onto the MUA implant analogs; Bottom: mandibular PMMA model with removable soft tissue frame and 4 SPG scanbodies screwed onto the MUA implant analogs.

For the stereophotogrammetric recording of implant positions, the Precise Implant Capture system (PIC Dental, Madrid, Spain) was used (see Fig. 1). The SPG ISBs were affixed onto the multiunit abutments, and the software recorded the specific SPG code associated with each implant site. The SPG camera was positioned at an angle of 45° and situated between 15 to 30 cm away from the model. The SPG device captured images, which were then processed through the SPG software to derive the three-dimensional coordinates of each implant in vector format. Subsequently, an .stl file was generated and exported.

III.1.3. Data processing and accuracy assessment

The alignment of the 60 test STL files with the reference scan was executed using specialized software (Geomagic Studio 12, 3DSystems, Rock Hill, SC, USA) with a precision of 0.01 mm for alignment tolerance. Two alignment optimizations were performed subsequent to file

superimposition. Employing the best fit method, the superimposition between scans of the test and control groups and the reference scan was achieved. This approach took into account only the implant positions for alignment, mimicking a typical clinical and laboratory workflow.

For evaluating the deviations, a best fit algorithm was adopted to gauge the variance of each implant in comparison to its counterpart in the reference file (Fig 4). This enabled a comprehensive analysis of the 3D linear and angular deviations for each implant, encompassing the distribution of errors across the three-dimensional coordinates.

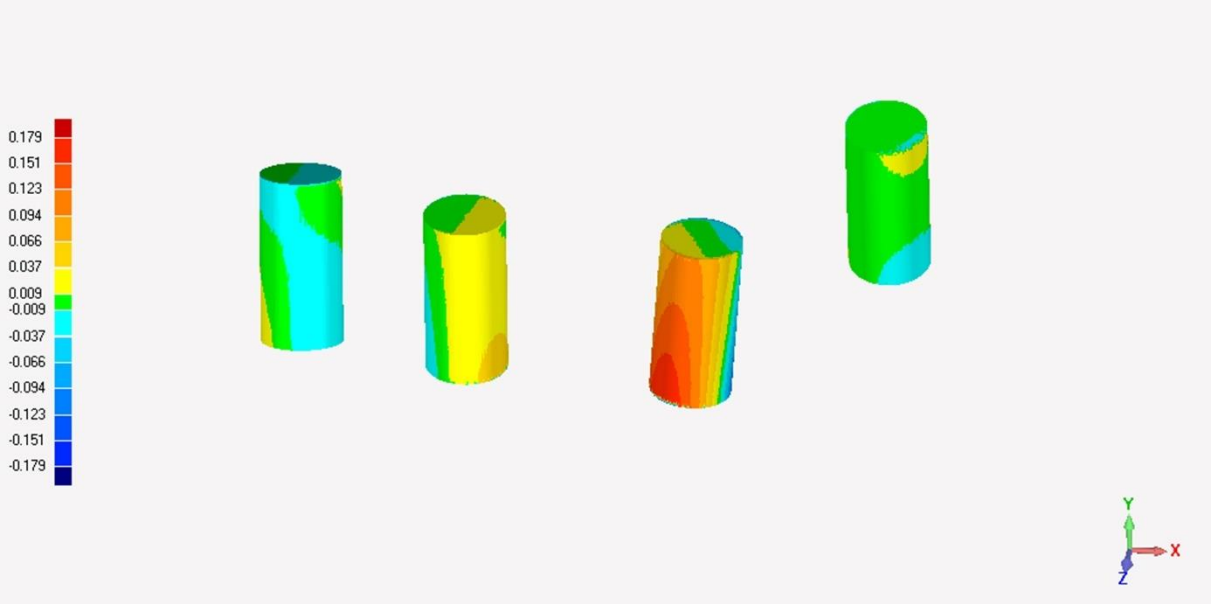

Fig.4: Alignment of the test files with the reference files in the four implant positions in Geomagic Studio (best fit algorithm).

Subsequently, dedicated measurement software (Hyper Cad S, Cam HyperMill, Open Mind Technologies, Milano, Italy) was employed to measure the linear (ΔX, ΔY, and ΔZ) and angular (ΔANGLE) discrepancies between each test scan and the reference scan for each analog. This measurement was conducted after reconstructing the linear geometries of the analogs, utilizing the centers of the digital analog heads as the reference points for deviation measurement.

Negative values along the X, Y, and Z axes indicated an ISB positioned to the left, downward, and backward, respectively, while positive values signified the opposite direction along each axis. The calculation of 3D deviations involved determining the Euclidean distance between the centers of the head of the test and control implant analogs (ΔEUC) [2, 5] (Fig. 5).

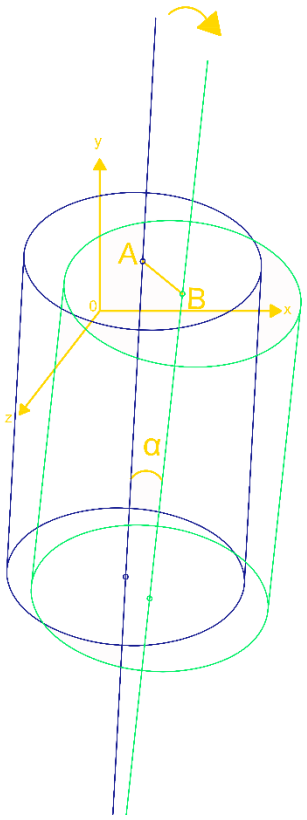

Fig.5: A schematic presentation of the measured parameters and the rationale of the analysis. Blue cylinder: the reference position of the implant analog. Green cylinder: the acquired position of the implant analog. A-B: linear deviation (the distance between the central points of the cylinder tops); α: angular deviation (the angle closed by the axes of the cylinders).

III.1.4. Statistical analysis

Assuming a significance level of 0.05 and considering ΔEUC as the primary endpoint, a sample size of 240 implants ensures a test power of 0.95 when considering a minimum expected difference of 20 μm. However, the calculation of the sample size was performed assuming an expected standard deviation of 40 μm for both IOS and SPG. While this assumption was consistent with the observed standard deviation for IOS, the observed variability in SPG was significantly lower. Therefore, a post hoc analysis based on observed values was conducted, yielding a statistical power of 0.98.

Continuous variables were characterized using mean, standard deviation, minimum, and maximum values. Kernel density estimates were employed to describe empirical distributions. To compare variances and expected values between two groups, Fisher's F test and T test were used, respectively. In cases where there were significantly different variances, Welch's t test was preferred.

III. 2. Methods of the clinical study

III.2.1. Ethical approval

This clinical trial received ethical approval from the University of Rome Tor Vergata's ethical committee (Protocol No. 203.20) and was officially registered as a clinical trial in the ISRCTN registry (Reg.No. ISRCTN12501259). The trial was conducted in accordance with the principles outlined in the Declaration of Helsinki as amended in 2008 and adhered to the tenets of GCP.

III.2.2. Recruitment and enrollment

Starting from November 2020, the clinical study aimed at recruiting and enrolling patients, aged 18 years or older, of both genders, who required complete arch fixed dental prostheses (FDPs).

Each enrolled patient provided informed consent after receiving detailed information about the study's nature, potential benefits, associated risks, and alternative treatment options. Moreover, patients were fully informed about any required follow-up assessments before being included in the study. The recruitment of patients continued in succession until April 2021, all of whom were treated at a single rehabilitation center.

The inclusion criteria encompassed the following: (1) Patients in good medical health; (2) Full-mouth bleeding and full-mouth plaque index equal to or below 25%; (3) Bone height supporting implants of a minimum length of 10 mm; (4) Bone width of at least 5 mm and 6 mm for narrow (NP 3.75 mm) and regular (RP 4.3 mm) implants, respectively; (5) Freshly extracted sockets displaying an intact buccal wall; (6) A minimum of 4 mm and 5 mm of bone extending beyond the root apex in the maxilla and mandible, respectively; (7) Minimal insertion torque of 45 Ncm; (8) A minimum mean value of 64 for ISQ (Implant Stability Quotient) on the day of the surgery; (9) Same-day surgery and provisionalization; (10) Screw-retained complete arch fixed dental prostheses (FDPs) anchored by 4 and 6 implants in the mandible and/or maxilla; (11) ISQ mean value of 72 on the day of the definitive impression; and (12) Availability to participate in regular follow-up appointments.

The exclusion criteria comprised several factors: patients classified as ASA (American Society of Anesthesiologists) class III or IV due to general medical conditions, or with psychiatric contraindications; individuals who were pregnant or breastfeeding; those under medication that could potentially interfere, such as steroid or bisphosphonate therapy; individuals with a history of alcohol or substance abuse; heavy smokers (consuming over 10 cigarettes per day); patients who had undergone radiation therapy to the head or neck region within the last 5 years; untreated periodontitis; acute and chronic infections affecting nearby tissues or natural dentition; individuals

with a significant maxillomandibular skeletal discrepancy; patients exhibiting high or moderate parafunctional activity; and those lacking opposing teeth, as per the criteria outlined by Johansson, Omar, and Carlsson [60].

III.2.3. Clinical and lab procedures

A single clinician executed all surgical and prosthetic procedures. Prior to the placement of implants, a comprehensive examination was administered to all participants in the study, which included a CBCT scan. The DICOM files resulting from the scan were imported into the implant planning software program (DTX Studio Implant, Dexis).

The implant planning process followed a meticulous approach that was both prosthetically and soft tissue driven. For the two anterior implants, a parallel positioning was ensured, while the 2 or 4 posterior implants were symmetrically angulated with consistent divergence compared to the anterior implants, in accordance with previous works [61-63].

Implant placement was carried out using conical connection implants (NobelActive, NobelParallel, NobelBiocare AG) with computer-assisted static and dynamic guided surgery methods [64]. An interim prosthesis made of digitally prefabricated multilayered polymethyl methacrylate (PMMA) (Whitepeaks, Whitepeaks Dental Solutions GmbH & Co.) was relined onto temporary cylinders that were screwed at the abutment level (MUA abutment, NobelBiocare AG). This interim prosthesis was delivered on the same day as the surgery. After a smooth healing period of 3 to 4 months, the provisional restoration was removed, and the implant stability quotient (ISQ) was evaluated.

In cases where the ISQ exceeded 72, abutment-level impression copings were securely fastened onto the multiunit abutments at a torque of 15 Ncm. A traditional definitive impression was then obtained using an open tray technique, employing plaster material (SnowWhite Plaster no. 2, Kerr) [11] (as depicted in Fig 6).

The conventional plaster impressions were utilized to create master casts, which were then digitally converted into high-resolution .stl files. This conversion adhered to ISO 12836 standards and involved the use of a laboratory scanner (D2000, 3shape) with a precision of 5 μm. These digital master cast .stl files were established as reference.

Fig. 6: The scalloped soft tissue ridge of the treated maxilla (top) and its traditional definitive impression in plaster (bottom).

The intraoral scans were performed using the TRIOS4 intraoral scanner (3Shape A/S), a wireless powder-free pen grip device utilizing confocal microscopy laser technology. The intraoral scanner was calibrated immediately prior to the scan. The scan employed implant scan bodies (Elos Accurate Multi-Unit; Elos Medtech) secured at the multiunit abutment level (Fig. 7). The scanning approach was consistent across all procedures, following the manufacturer's guidelines, and initiated from the furthest ISB on the patient's left side.

The SPG system (Precise Implant capture, PIC camera, PIC dental) utilized two CCD cameras designed for clinical use to identify surface-encoded scan bodies secured onto the multiunit abutments (Fig. 8). As discussed under I.2., these cameras capture 10 extraoral photographs per second with an error margin < 10 µm. Before the scan, the SPG scanbodies were identified according to their surface code, registered in the software, and screwed onto the multiunit abutments.

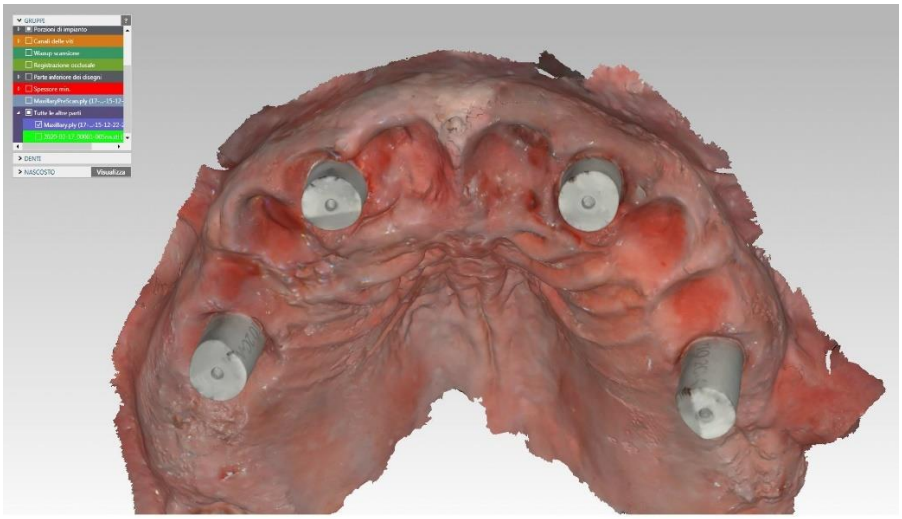

Fig.7: Intraoral scan (TRIOS 4) with four Elos Accurate Multi-Unit abutments secured at the multiunit abutment level.

Fig.8: Preparation for SPG scanning: the SPG camera and the characteristic flag-like scanbodies in a patient's mouth.

The SPG system was positioned outside the patient's mouth, approximately 15 to 30 cm away, at variable angles between 90° and 45° with respect to the scan body surface. This ensured comprehensive visibility of all SPG scan body geometries to the stereo cameras (Fig.9).

Following internal system calibration, the captured SPG system images underwent processing. The software algorithm extracted the relative angles and distances between each implant position

in vector form. The outcome of the SPG impression was an STL file that exclusively represented the vectorial relationship among the implant prosthetic platforms (Fig.10).

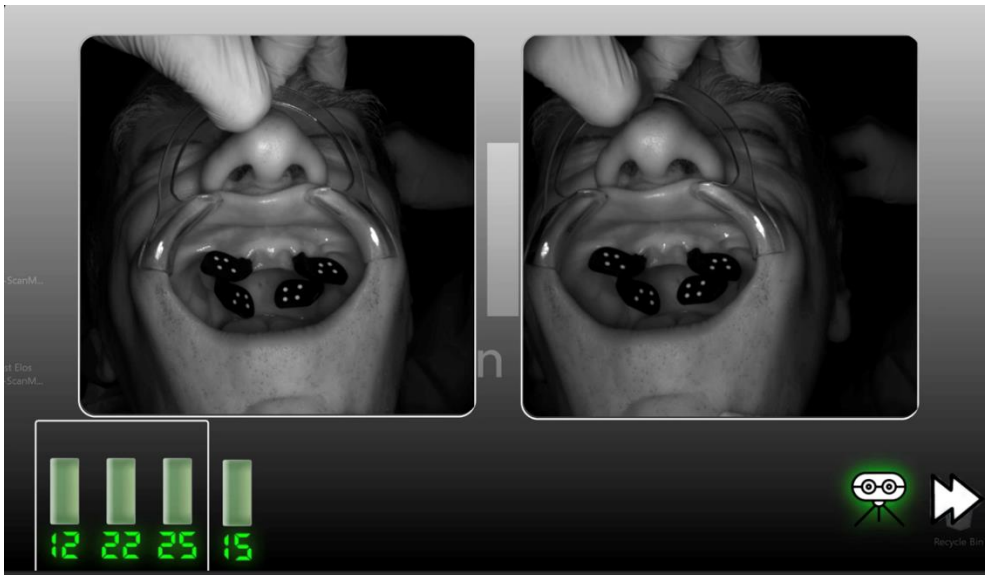

Fig.9: The scan bodies as seen and identified by the SPG system. The numbers in the bottom left corner indicate the tooth positions associated with each scan body.

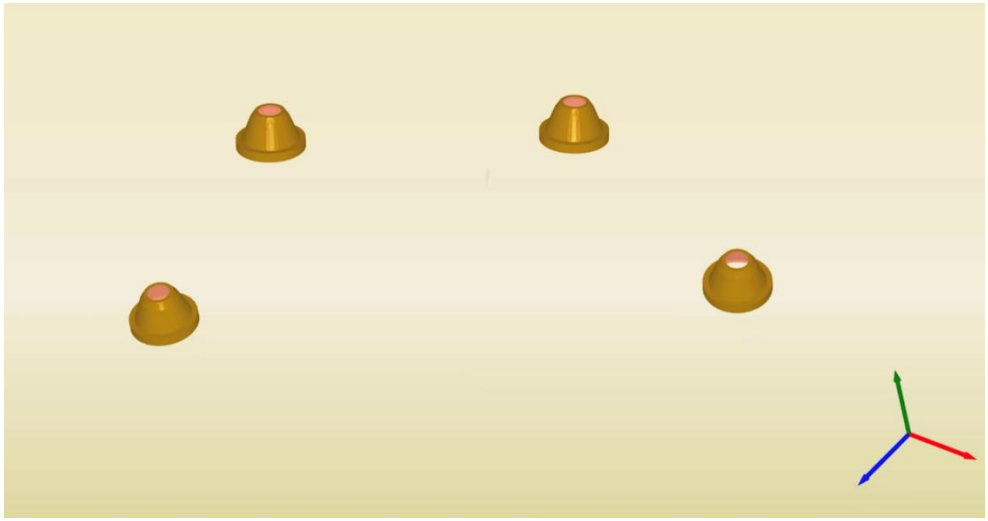

Fig.10: The outcome of the SPG impression: the vectorial relationship among the implant prosthetic platforms.

To complete the overall information, this SPG data needed to be merged with the soft tissue details acquired from the IOS impression. This integration was achieved using a best-fit software algorithm (DTX StudioLab, Dexis).

Zirconia-based complete arch fixed dental prostheses (ISZ-FDPs), supported by implants and retained with screws, were digitally designed using master cast reference files. These reference files were obtained from plaster impressions and the ISZ-FDPs were subsequently manufactured through centralized industrial production (NobelBiocare Procera LL), as illustrated in Figure 11.

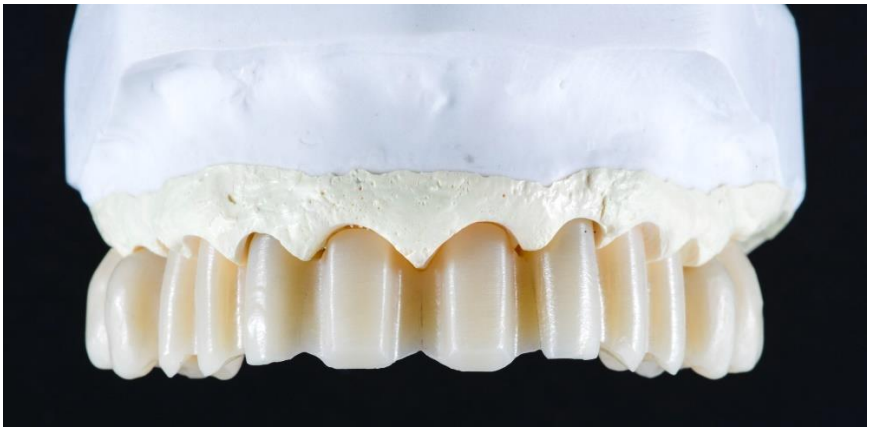

Fig.11: An implant-supported, screw-retained, zirconia-based, complete-arch fixed prosthesis from the study placed on the master cast for fit assessment.

To evaluate precision and fit, the ISZ-FDPs were initially examined on their respective master casts using a dental laboratory microscope (Leica M50, Leica Microsystems) at 35x magnification. This assessment was complemented by the Sheffield one-screw test. Subsequently, clinical evaluations were conducted in the patient's mouth, adhering to established criteria. These criteria included strain-free screwing and the absence of open margins, both confirmed during the chair-side Sheffield one-screw test. This examination encompassed close-up inspections and periapical radiographs, ensuring the proper placement of the framework without vertical or horizontal discrepancies. The evaluation standards drew from well-regarded references in the field, including studies by Abduo et al. [65], Kan et al. [66], and Pozzi et al. [11, 49].

III.2.4. Data processing and accuracy assessment

The accuracy and fit assessment yielded successful results for all ISZ-FDPs. For every patient's full arch, three digital files were procured: one served as a reference scan, achieved through the indirect digitalization of the plaster impression, and two functioned as test scans (obtained through IOS and SPG digital impressions). These digital files exclusively encompassing the implant positions were subsequently employed for the precision analysis.

The test scans acquired from both IOS and SPG methods for each patient's complete arch were meticulously aligned to the corresponding reference scan utilizing a best-fit algorithm (Geomagic Studio 12, 3DSystems, Rock Hill, SC, USA). The alignment process adhered to a tolerance of 0.01 mm, and two alignment optimizations were performed post file superimposition.

Linear discrepancies (ΔX, ΔY, and ΔZ) as well as angular variations (ΔANGLE) between the test scan and reference scan were meticulously measured for every implant position. The analysis involved scrutinizing the previously superimposed files utilizing dedicated software (Hyper Cad S, Cam HyperMill, Open Mind Technologies, Milano, Italy). In terms of the X, Y, and Z axes, negative values indicated an implant situated towards the left, downward, and backward respectively (denoting lateral, vertical, and longitudinal directions). Conversely, positive values represented the opposing direction along each axis. A comprehensive three-dimensional (3D) deviation was then calculated for each implant position, employing the Euclidean distance (ΔEUC) as the determining factor.

III.2.5. Statistical analysis

For the statistical analyses, SAS 9.4 (SAS Institute, Cary, NC, USA) and R 3.4. (R Development Core Team).

Taking Euclidean distance as the primary endpoint, setting the level of significance at p= 0.05, and assuming a paired t-test, a minimum sample size of n=84 was deemed necessary. This sample size was calculated to ensure a test power of 0.95, with a minimum anticipated difference of 120 µm (alongside a standard deviation of 150 µm).

To describe continuous variables, mean, standard deviation, minimum, and maximum values were reported. Discrepancies between errors associated with the two devices (SPG - IOS) were determined for each implant. Negative values denoted a favorable accuracy outcome in favor of SPG. Kernel density estimator was employed to derive their empirical distributions, and the evaluation of significance was carried out through a paired t-test. For the analysis of the intergroup differences, ANOVA was employed.

Multivariate analysis was undertaken through the application of a mixed linear model. Two distinct models were established, with ΔEUC and ΔANGLE serving as dependent variables. To enhance normality, a logarithmic transformation was applied. Both models incorporated fixed effects including the scanning device (IOS vs SPG), type of arch (maxilla vs mandible), and the number of supporting implants (4 implants vs 6 implants).

IV. RESULTS

IV.1. Results of the *in vitro* study

Deviation analysis involved comparing the reference scan with 60 test scans (30 IOS, 30 SPG) for each of the 240 implant analogs. This assessment encompassed deviations along the X, Y, and Z-axes, as well as angular discrepancies. The linear disparities were utilized to compute the 3D deviation using ΔEUC, irrespective of error direction. Detailed deviations from the reference scan for both IOS and SPG are outlined in Table 1. Notably, IOS exhibited elevated 3D mean ΔEUC in comparison to SPG (52.8 µm vs. 33.4 µm, $p<0.0001$), with extreme values reaching up to 181.9 µm. It is pertinent to mention that IOS displayed a significantly higher standard deviation (SD) compared to SPG (37.1 µm vs. 17.7 µm, $p<0.0001$). Exploring ΔANGLE, IOS exhibited slightly higher mean deviations than SPG (0.28° vs. 0.24°, $p=0.0022$), featuring extreme measurements of up to 0.73°.

Table 1. Descriptive analysis of the linear, 3D, and angular deviations broken down by the applied digital impression technology.

	IOS			SPG		
	Mean	**SD**	**Range**	**Mean**	**SD**	**Range**
ΔY (µm)	-2.03	14.54	(-71.86, 18.77)	0.95	7.15	(-13.09, 18.42)
ΔX (µm)	5.21	50.51	(-87.29, 146.55)	12.81	19.23	(-52.86, 51.67)
ΔZ (µm)	-1.85	37.31	(-117.53, 82.95)	20.78	20.42	(-43.16, 75.97)
ΔEUC (µm)	52.81	37.11	(4.18, 181.88)	33.42	17.71	(7.56, 80.34)
ΔANGLE (°)	0.28	0.14	(0.03, 0.73)	0.24	0.04	(0.15, 0.36)

Abbreviations: IOS: intraoral scanning; SPG: stereophotogrammetry; SD: standard deviation.

The SD values for SPG were notably smaller than those for IOS (0.14° vs. 0.04°, $p<0.0001$). Tables 2 and 3 delineate 3D and angular discrepancies categorized by implant position and scanning device, while empirical distributions are presented in Figures 12 and 13. For ΔEUC, implant site 45 emerged as the most critical when scanned with IOS (deviations up to 181.88 µm), whereas anterior implants (42 and 32) were more sensitive to SPG scanning. The reduction in 3D variability was significantly more prominent for SPG across all implants, except 42, where the reduction did not reach statistical significance. No notable mean difference was discerned between the two devices for implant 42. Figure 12 illustrates the comparable performance of IOS and SPG for the anterior implant 42, whereas a distinct advantage of SPG is evident for posterior implants (45 and 35), particularly for implant 45. Regarding ΔANGLE, marginal discrepancies were

identified related to implant position. The anticipated angular discrepancy differed significantly between IOS and SPG only for implant 42 (0.40° vs. 0.23°, p<0.0001). However, it is noteworthy that SPG consistently exhibited superior performance to IOS in terms of SD.

Table 2: 3D distances (ΔEUC, µm) stratified for implant position and scanning device. F test and T test were used to compare variances and expected values between two groups (IOS and SPG).* *P*-value from the Welch T-test. The conventions are the same as in Table 1.

	IOS			SPG				
Implant	**Mean**	**SD**	**Range**	**Mean**	**SD**	**Range**	**F test *P*-value**	**T test *P*-value**
45	81.85	48.22	(15.72, 181.88)	29.25	3.73	(17.57, 35.41)	<0.0001	<0.0001*
42	43.46	22.43	(10.82, 81.59)	48.58	19.37	(15.36, 80.34)	0.4350	0.3474
32	56.14	27.17	(5.07, 103.18)	41.06	14.41	(22.54, 77.18)	0.0010	0.0102*
35	29.79	23.73	(4.18, 107.22)	14.78	3.83	(7.56, 22.51)	<0.0001	0.0018*

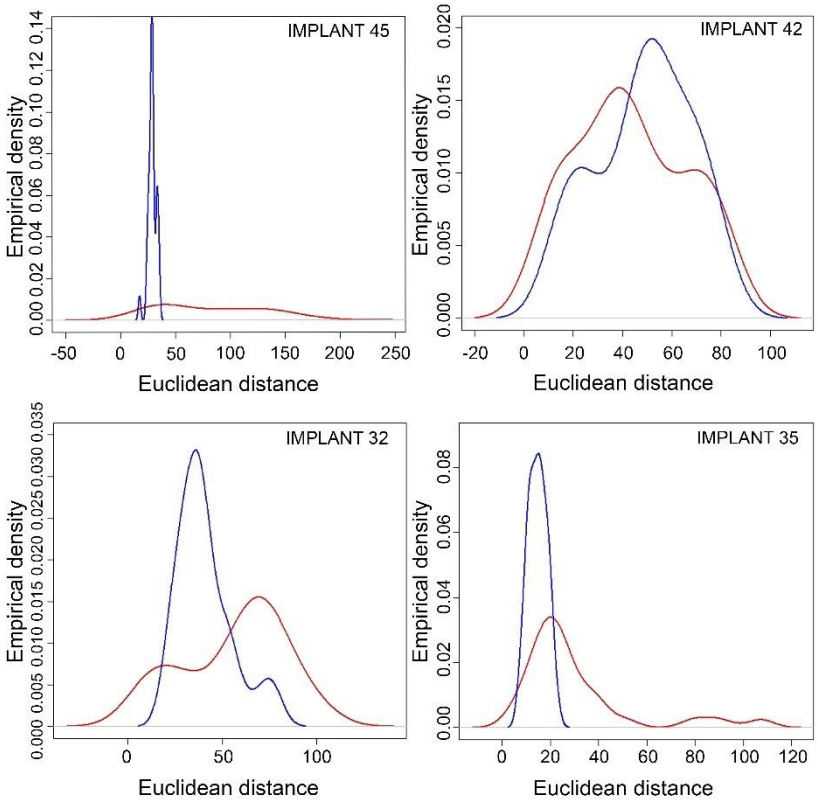

Figure 12: Empirical distributions of ΔEUC stratified for implant position and scanning device (red: IOS, blue: SPG)

Table 3: Angular discrepancies (ΔANGLE, °) stratified for implant position and scanning device. F test and T test were used to compare variances and expected values between two groups (IOS and SPG). * *P*-value from the Welch T-test. The conventions are the same as in Table 1.

	IOS			SPG				
Implant	**Mean**	**SD**	**Range**	**Mean**	**SD**	**Range**	**F test *P*-value**	**T test *P*-value**
45	0.29	0.13	(0.08, 0.73)	0.29	0.05	(0.19, 0.36)	<0.0001	0.8719*
42	0.40	0.13	(0.15, 0.67)	0.23	0.02	(0.20, 0.27)	<0.0001	<0.0001*
32	0.21	0.11	(0.03, 0.41)	0.24	0.02	(0.20, 0.29)	<0.0001	0.1820*
35	0.24	0.12	(0.09, 0.52)	0.21	0.03	(0.15, 0.26)	<0.0001	0.1728*

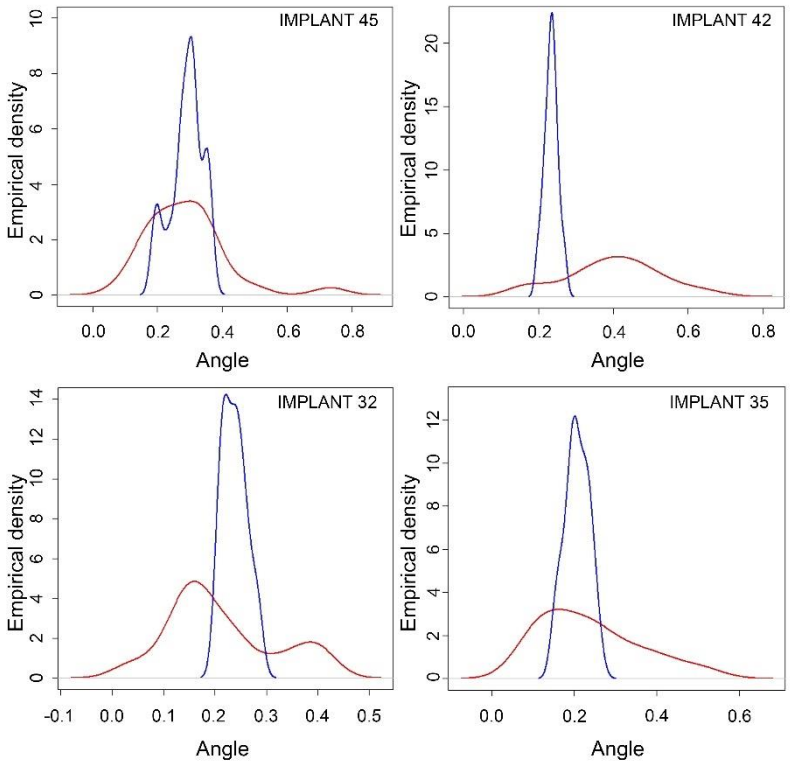

Figure 13: Empirical distributions of ΔANGLE stratified for implant position and scanning device (red: IOS, blue: SPG)

IV.2. Results of the clinical study

Eleven patients with edentulous arches underwent rehabilitation with screw-retained implant prostheses, with 5 cases involving maxillae and 6 involving mandibles. A total of 50 implants were employed, supported by either 4 (n=8) or 6 implants (n=3). In total, 100 implant positions were scanned using two digital devices (IOS and SPG) and compared to reference scans. The comprehensive breakdown of deviations from reference scans for both IOS and SPG is shown in Table 4.

Table 4: Descriptive analysis of the linear, 3D, and angular deviations stratified by the applied digital impression technology.

	Mean	SD	Min.	Max.
		IOS		
Δx (μm)	-19.8	110.2	-223	304.7
Δy (μm)	-4.1	44.3	-111.6	-147.1
Δz (μm)	-41.9	127.5	-536.3	177.6
ΔEUC (μm)	137.2	115.5	11.5	558.1
ΔANGLE (°)	0.79	0.59	0.05	2.89
		SPG		
Δx (μm)	-24.8	71.8	-192	113.8
Δy (μm)	-3.4	29	-173.8	50.8
Δz (μm)	20.9	79.1	-264	250.8
ΔEUC (μm)	87.6	74.2	12	316.2
ΔANGLE (°)	0.38	0.29	0.02	1.92

It is noteworthy that, with the exception of ΔX, mean errors associated with SPG were consistently lower than those linked to IOS. A notable discrepancy can also be observed in terms of standard deviation, favoring SPG for both linear and angular deviations. For each implant, the discrepancy between ΔEUC values associated with the two devices (SPG - IOS) was computed, leading to an empirical distribution represented in Figure 10. This analysis revealed a mean difference of -49.60 μm (SD 138.15), indicating a significant reduction in errors for SPG compared to IOS ($p = 0.0143$). The distribution of differences was further stratified based on arch type and implant number, depicted in Figure 11. Notably, the sample lacked mandibles with 6 implants. While no significant disparity was identified among the three groups ($p = 0.5925$), notable differences were observed for mandibles with 4 implants, displaying marked advantages for SPG (Table 5).

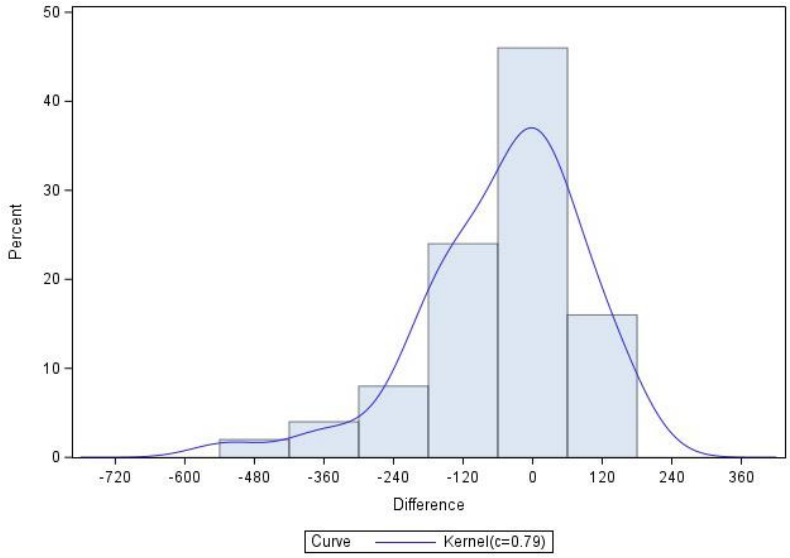

Fig.10: Empirical distribution of ΔEUC difference between stereophotogrammetry and intraoral optical scanning.

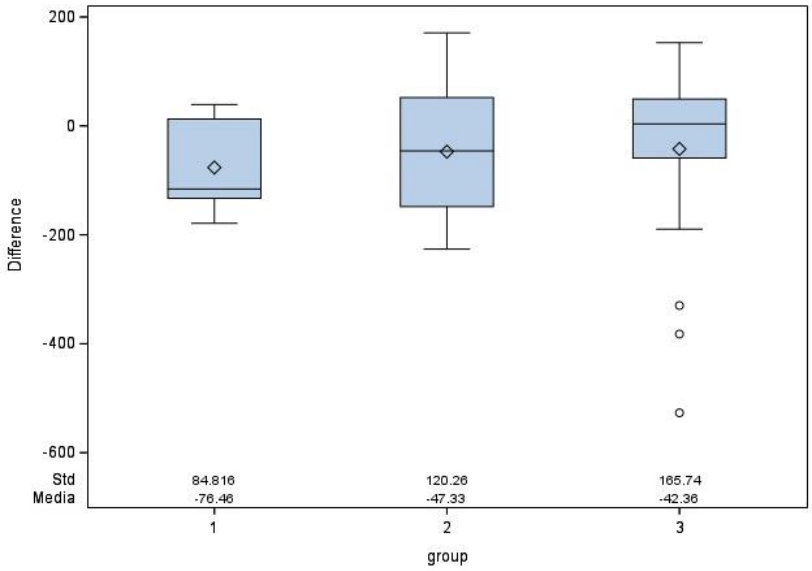

Fig.11: Distribution of ΔEUC difference between stereophotogrammetry and intraoral optical scanning according to type of arch and implant number: 1=maxilla with 4 implants, 2= maxilla with 6 implants, 3= mandible with 4 implants.

Table 5: Extreme cases of ΔEUC deviation (μm)

Observation No.	SPG	IOS	Difference	Arch	Support
24	31.2107	558.082	-526.871	mandible	4 implants
31	30.1874	359.980	-329.793	mandible	4 implants
39	25.7195	407.929	-382.209	mandible	4 implants

Turning attention to the ΔANGLE distribution (Fig. 12), an average deviation difference of -0.40° (SD 0.65°) was observed, signifying a significantly positive impact of SPG ($p < 0.0001$). Upon stratified analysis, no noteworthy distinctions were found among the groups ($p = 0.2666$) (Fig 13). Of particular interest are the three instances of extreme angular accuracy differences, strongly favoring SPG at approximately -2.75, -1.90, and -1.62° (Table 6).

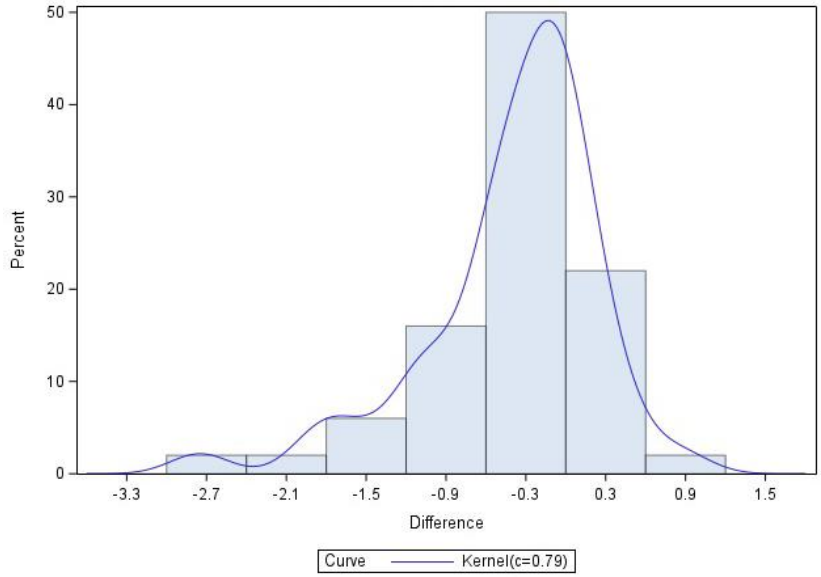

Figure 12: Empirical distribution of ΔANGLE difference between stereophotogrammetry and intraoral optical scanning.

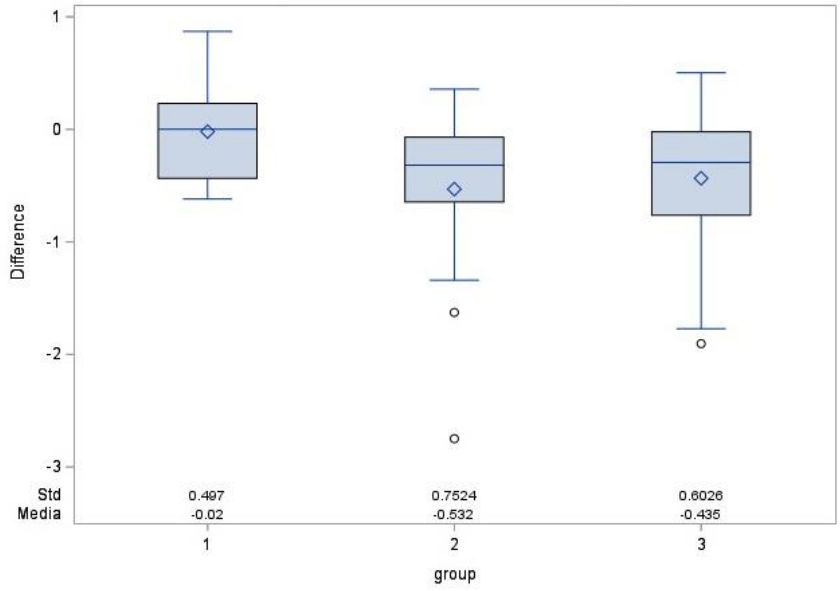

Figure 13: Distribution of ΔANGLE difference between stereophotogrammetry and intraoral optical scanning according to type of arch and implant number: 1=maxilla and 4 implants, 2= maxilla and 6 implants, 3= mandible and 4 implants.

Table 6: Extreme cases of ΔANGLE deviation (°).

Observation No.	SPG	IOS	Difference	Arch	Support
16	0.1419	2.8905	-2.7486	maxilla	6 implants
25	0.4563	2.0836	-1.6273	maxilla	6 implants
31	0.1397	2.0441	-1.9044	mandible	4 implants

The multivariate analysis employed two distinct mixed linear models, with ΔEUC and ΔANGLE as dependent variables. Both models considered the scanning device (IOS vs SPG), arch type (maxilla vs mandible), and implant number (4 implants vs 6 implants) as independent variables. Notably, the scanning device exhibited a significant impact on both ΔEUC and ΔANGLE, with p-values of 0.0162 and 0.0001, respectively (Tables 7 and 8). Conversely, no significant effects were detected for arch type or implant number. It is pertinent to highlight that, for ΔANGLE, parameter estimates for arch type and implant number are close to 0, while for ΔEUC, the estimated effects and standard errors remain consistent.

Table 7: Estimates of fixed effects on ΔEUC (logarithmic scale).

Effect	Estimate	SE	t-value	F-value	*p*-value
Intercept	4.28	0.29	-	-	-
Device (PSG vs IOS)	-0.42	0.17	-2.45	6.02	0.0162
Type of arch (Mandible vs Maxilla)	0.31	0.32	0.98	0.96	0.3294
Implant number (6 vs 4)	0.36	0.34	1.06	1.12	0.2926

Table 8: Estimates of fixed effects on ΔANGLE (logarithmic scale).

Effect	Estimate	SE	t-value	F-value	*p*-value
Intercept	-0.55	0.20	-	-	-
Device (SPG vs IOS)	-0.67	0.15	-4.48	20.10	<0.0001
Type of arch (Mandible vs Maxilla)	0.03	0.22	0.12	0.01	0.9067
Implant number (6 vs 4)	0.10	0.23	0.42	0.18	0.6755

V. DISCUSSION

This thesis is founded on two investigations: an *in vitro* study and a clinical study. Both inquiries aimed to assess the precision of stereophotogrammetry when used for obtaining comprehensive digital impressions of complete arches, in comparison with intraoral scanning.

In our *in vitro* study, we scrutinized and juxtaposed the accuracy of the two digital impression techniques, namely intraoral scanning (IOS) and stereophotogrammetry (SPG), for capturing complete arch implant impressions. The analysis encompassed evaluating the trueness and precision of both IOS and SPG, measured through linear and angular deviations, respectively. The study design was constructed upon utilizing a best-fit alignment technique between the reference and test scans, aimed at quantifying deviations for each implant position and subsequently examining the 3D deviations along the three spatial axes. The best-fit algorithm facilitated the assessment of deviation for all implant positions through a comparison of corresponding test and reference files. This approach enabled a comprehensive analysis of implant deviations from linear (ΔY, ΔX, ΔZ), 3D (ΔEUC), and angular (ΔANGLE) perspectives.

The Euclidean distance, serving as a metric for 3D deviation, was chosen over the root mean square (RMS) due to its greater practical applicability as a clinical outcome measure. The rationale behind selecting a certified 5 μm accuracy optical desktop scanner as the reference was grounded in its enhanced accessibility to the freedom plane in comparison to tactile systems like the coordinate measuring machine (CMM) [67].

The null hypothesis was refuted due to the superior performance of SPG over IOS in terms of both 3D trueness (ΔEUC) and precision. This trend was further evident when examining angular deviations (ΔANGLE), where SPG outperformed IOS in both angular trueness and precision.

Regarding 3D mean deviations (ΔEUC), IOS exhibited higher values compared to SPG (52.8 μm vs. 33.4 μm, $p < 0.0001$), with instances of extreme measurements reaching up to 181.9 μm. Notably, the standard deviation (SD) associated with IOS was significantly elevated compared to SPG (37.1 μm vs. 17.7 μm, $P < 0.0001$).

As for angular deviations (ΔANGLE), IOS displayed slightly elevated mean deviations in contrast to SPG (0.28° vs. 0.24°, $p = 0.0022$), with extreme measurements reaching up to 0.73°. It is worth noting that the SD values for SPG were notably lower than those for IOS (0.14° vs. 0.04°, $p < 0.0001$).

The study results were consistent with the findings of a recent *in vitro* study by Tohme et al., where they assessed and compared the scan body coordinates of the reference cast against the scan body positions acquired through conventional (impression plaster), IOS, and SPG techniques [68]. The authors utilized the same SPG device as employed in the current study, along with a desk scanner featuring a precision of 7 μm as the reference standard. Additionally, the study conducted an analysis of global angular distortion and 3D deviations for both the entire scan body and the flat-angled surface, employing an inspection and metrology software program in combination with the best-fit alignment approach. Despite differences in methods and the IOS utilized when compared to the present study, the SPG technique demonstrated the highest levels of accuracy in terms of trueness and precision for the intraoral scan bodies across all evaluated techniques.

Another *in vitro* study conducted a comparison of accuracy among a conventional technique (elastomeric impression), SPG, and two IOSs, utilizing a Coordinate Measuring Machine (CMM) with a nominal linear accuracy of 1 μm as the reference standard. Strikingly different outcomes were observed [39]. The SPG system (iCam4D; Imetric4D Imaging Sárl, Courgenay, Switzerland) exhibited the least accurate measurements, displaying the highest 3D discrepancy for implant positions across all groups, with an average 3D deviation of 77.6 μm.

Similarly, a different study evaluated the accuracy of conventional techniques (polyether impression) as well as SPG and IOS for complete-arch implant impressions, utilizing a laboratory scanner with a precision of 4 μm as the reference [57]. Employing a best-fit algorithm, the test and control files were superimposed, and the 3D discrepancy between the two STL files was assessed using Root Mean Square (RMS) error through inspection software. The SPG method demonstrated the least 3D discrepancy concerning trueness and precision for implant abutment positions, while the IOS exhibited the lowest accuracy among the three impression techniques tested.

It is worth noting that the two previously mentioned studies investigated the same SPG system (iCam4D; Imetric4D Imaging Sarl, Courgenay, Switzerland), albeit employing different reference systems (desk scanner) and employing distinct measurement analyses (RMS). These variations in study designs account for the conflicting results observed.

In this study, the IOS exhibited elevated 3D mean deviations compared to SPG (52.8 μm vs. 33.4 μm, $p < 0.0001$), reaching extreme measurements of up to 181.9 μm. Upon dissecting the 3D deviation across the three spatial axes, IOS displayed heightened deviations along the X-axis (lateral) at 5.21 ± 50.51 μm, while SPG demonstrated notably accurate performance on the Y-axis (vertical) at 0.95 ± 7.15 μm. Note that the extreme deviation values observed with IOS in this

study surpassed the clinically acceptable misfit threshold of 150 μm, which is recommended to avert potential long-term mechanical and biological complications [10, 69, 70].

Regarding angular deviations, the IOS exhibited slightly greater mean deviations than the SPG (0.28° vs. 0.24°, p = 0.0022), with extreme measurements extending up to 0.732°. These high angular deviations associated with IOS may potentially have adverse implications for the overall fit of implant-prosthesis assemblies, particularly notable in the context of screw-retained complete-arch restorations.

When exploring 3D deviations according to implant position, it becomes evident that implant 45 assumes a pivotal role in the scanning process, displaying IOS deviations reaching up to 181.87 μm. Conversely, anterior implants 42 and 32 garner heightened significance for scanning via the SPG, featuring deviations of up to 80.34 μm and 77.18 μm, respectively.

It is important to acknowledge the inherent constraints of optical surface scanning technology, which necessitates the adoption of a consistent and precise scanning trajectory to minimize the need for image capture and stitching procedures. As a result, strict adherence to the manufacturer's guidance for the evaluated IOS is paramount, with the scanning process commencing from the farthest implant and proceeding in sequence along the dental arch, either left to right or right to left.

For the purpose of facilitating subsequent comparisons, we adopted a previously published scanning strategy [2, 59]. The scanning process commenced with the occlusal-lingual surface of the ISB at position 45 and subsequently progressed along the arch, covering positions 42, 32, and 35. Later, the scanning procedure was reversed, starting from the occlusal-buccal aspect. Notably, while the customary IOS starting point tends to exhibit enhanced trueness and accuracy, the present study identified position 45 as critical, as it was the most complex point concerning depth and angulation (depth, -4 mm; distal angulation, 15°), which is in agreement with previously documented findings [19].

With the exception of implant 42, the SPG device exhibited a notable decrease in 3D variability in comparison to the IOS device across all implants. Notably, no significant disparities emerged between the two devices for implant 42. These findings validate the heightened accuracy of the SPG, despite a marginal decrease in precision observed for anterior implants in both trueness and precision aspects. This decline in accuracy for the anterior implant positions led to a similar or higher level of accuracy compared with the IOS. It is assumed that the inferior SPG performance in the anterior implants, compared to the posterior implants, may be attributed to the way the model was scanned.

The ideal scanning orientation of the SPG device, with reference to the coronal plane, should closely match the orientation of the dedicated ISB flags attached to the implant. This alignment should consider both the bucco-lingual and mesio-distal aspects. This alignment aims to enable the simultaneous capture of implant coordinates during the scanning process. In clinical practice, achieving this alignment involves having the patient open their mouth, allowing the lip retractor to expose all flags for visualization using the two infrared stereocameras. However, a challenge arises with anterior implant flags potentially obstructing the view of posterior ones. To strike a balance, it is suggested to maintain a scanning angle of approximately 45 degrees during mouth opening. In our in vitro study, the influence of the angle at which the mouth is opened was not taken into account. Instead, the simulation involved attaching the model to a flat surface with a fixed 45-degree orientation. From this, one can deduce that applying the suggested in vivo scanning angle of 45 degrees to a model positioned parallel to the horizontal plane could have resulted in variations in the outcomes of the laboratory study.

Angular deviation was independent of implant position, regardless of whether IOS or SPG was applied, except for implant 42, where a significant difference was found between IOS and SPG (0.40° vs. 0.23°, $p < 0.0001$). However, SPG consistently demonstrated notably improved performance over IOS in terms of standard deviation (SD). Consequently, despite the *in vitro* setting that might have favored IOS surface scanning, SPG exhibited greater accuracy in both 3D and angular measurements. This outcome likely stems from the distinct technologies employed by the two devices.

The IOS software utilizes a process called "stitching" to elaborate and align the acquired 3D images, employing a best-fit algorithm. This stitching procedure, repeated for each image pairing, contributes to the deviation associated with image coupling. The magnitude of stitching-related error increases with the number of image stitches, thus elevating the overall alignment error [26]. On the other hand, SPG operates as an extraoral device equipped with two infrared charge-coupled device cameras that simultaneously detect specific optical landmark geometries encompassing the surface of each ISB flag. This approach records implant coordinates and their spatial relationships in terms of distances and angulations [47]. Due to its broader field of view, unlike the currently available IOS devices, SPG captures all implant coordinates and spatial relationships without requiring stitching procedures, thus eliminating this source of error.

In addition, the extraoral scanning method employed by SPG ensures immunity to the confounding factors of IOS documented in existing literature. These factors include patient's mouth opening, size of the scanner tip, saliva, steam, the material composition of the scan bodies, their distance,

and the extent of the edentulous span and arch. Moreover, SPG's infrared technology remains unaffected by ambient light or light reflections [51].

Furthermore, there was a significantly higher standard deviation (SD) associated with IOS, both in terms of 3D deviation (37.1 μm vs. 17.7 μm, $p < 0.0001$) and angular deviation (0.14° vs. 0.04°, $p < 0.0001$). Based on the SD values for 3D and angular deviations, SPG exhibited considerably greater precision compared to IOS. This demonstrates the superior recording repeatability of SPG, a phenomenon potentially attributed to the distinct scanning procedures associated with the two digital impression devices. The IOS necessitates adequate movement by the clinician along the arch, adhering to a well-defined scanning strategy, in order to capture all ISB positions and the encompassing gingival anatomy. This approach facilitates swift and precise stitching of the acquired 3D images. In contrast, SPG functions as an extraoral digital device, obviating the need for movement along the arch. Instead, only minor adjustments are required to accurately focus on the SPG scan body geometry [6]. Consequently, operator influence is more pronounced when employing the IOS, potentially contributing to diminished consistency in measurement procedures.

It is of utmost importance to emphasize that the conclusions derived from this study are applicable solely to the examined IOS and SPG systems, and therefore, should be thoughtfully extended to alternative devices. It is noteworthy that the scans were conducted by a single proficient clinician, with previous investigations suggesting negligible operator impact on IOS accuracy [2]. Additional research endeavors are merited to probe into the operator's influence and the learning curve associated with SPG technology, an area currently devoid of comprehensive information in the existing literature.

However, the primary limitations of this study originate from its *in vitro* context, which could potentially lead to an underestimation of deviations attributed to patient-related elements such as saliva, blood, tongue, and movements [20]. In response to this concern, we also addressed identical inquiries within a clinical study.

The utilization of full-arch digital implant impressions remains a subject of debate due to the limited existing data, as evidenced by just a pair of *in vivo* investigations that have contrasted SPG and IOS technologies [15, 71]. The principal aim of our single cohort clinical trial was to scrutinize and juxtapose the precision of IOS and SPG in capturing complete-arch digital implant impressions. A secondary objective encompassed an examination of the potential impact exerted by the arch type (maxilla vs. mandible) and the number of implants (4 vs. 6) on the accuracy of SPG and IOS methodologies.

To our current knowledge, this is the first clinical trial to evaluate the precision of complete-arch digital impressions utilizing two devices operating according to different principles and incorporating meticulous sample size determination and robust statistical analysis. As it is the first study of this kind, calculating a proper sample size was not an easy task. Assuming the primary endpoint as Euclidean distance and a significance level of p= 0.05, a minimum sample size of n = 84 was computed, ensuring a minimum anticipated variance of 120 (±150) μm and a statistical power of 0.95. During the progression of the study, the total sample size was elevated to n = 100 (adding up to 50 implant positions per device). This encompassed the assessment of 11 complete arches (5 maxillae and 6 mandibles) in 11 patients. The evaluation adhered to the tenets of good clinical practice and meticulous documentation, with no instances of protocol deviations. Each participant enrolled in the study underwent three impressions (plaster, SPG, and IOS). The comparative assessment of IOS and SPG clinical efficacy encompassed a paired analysis of deviation disparities for every implant position.

The utilization of a certified optical desk scanner with a 5 μm accuracy, despite its limitations, was justified due to its enhanced accessibility to freedom planes in contrast to tactile systems like the coordinate measuring machine. Furthermore, this approach is widely accepted as a laboratory practice for digitizing plaster master casts [67].

The study's methodology was structured around the application of a Gauss best-fit alignment algorithm to establish optimal congruence between reference and test scans. This algorithm was employed to quantify the deviations at each implant location and subsequently to evaluate the three-dimensional deviations along the three spatial axes. Referred to as the iterative closest point alignment, the Gauss best-fit algorithm enabled the comprehensive assessment of deviation across all implant positions by comparing the respective test and reference files. Its efficacy as a measurement technique surpasses that of alternative alignment algorithms, as demonstrated by Peroz and co-workers [72]. This approach facilitated a comprehensive analysis of each implant's deviations from linear (ΔY, ΔX, ΔZ), three-dimensional (ΔEUC), and angular (ΔANGLE) perspectives.

The null hypothesis was refuted since SPG exhibited superior performance compared to IOS, both concerning 3D (ΔEUC) ($p = 0.0143$) and angular deviations (ΔANGLE) ($p < 0.0001$), with no detected influence from arch type (maxilla vs. mandible) or implant count (4 vs. 6) on SPG and IOS accuracy. While previous research has assessed various IOSs for complete-arch implant impressions, a consensus has yet to be reached regarding the practicality of this technique in daily practice [18, 73-75]. Presently, agreement is lacking on the acceptable misfit range and the

appropriate clinical measurement of misfit [7, 76]. Nevertheless, a suggested threshold of 150 μm aims to prevent long-term complications such as retention loss, screw loosening, framework fracture, or veneering material damage [4, 69, 77]. Furthermore, extreme values for 3D and angular deviations of a single implant in a complete arch supported by 4 and 6 implants were established as 150 and 50 μm in horizontal and vertical dimensions and 1° in angulation [78]. Additionally, with an increasing number of implants, the allowable error tolerance in the three axes and angulations decreases [79].

Additionally, it is crucial to take into account the manufacturing tolerances of prosthetic suprastructures, which can lead to misfits in the form of gaps ranging from 20 to 100 μm [80]. A recent *in vitro* study that investigated the same SPG device suggested that SPG could potentially serve as a clinically acceptable alternative to traditional complete-arch implant impressions. However, when compared to a splinted elastomeric impression method, the latter exhibited statistically significantly higher overall accuracy. The trueness difference between the systems was 3 μm, while the precision difference was 18 μm [58].

In the current investigation, the average errors linked to SPG usage consistently remained lower than those associated with IOS, except for the lateral axis (ΔX). The most notable variance was observed along the longitudinal axis (ΔZ), wherein SPG exhibited a deviation of 20.9 (±79.1) μm, while IOS displayed a deviation of -41.9 (± 127.5) μm. Furthermore, the overall three-dimensional deviations across the three axes strongly favored SPG, measuring 87.6 μm (± 74.2) in contrast to IOS's 137.2 (± 115.5) μm. These values were notably below the accepted threshold necessary for achieving a favorable long-term clinical prognosis for complete-arch implant-supported prostheses. In terms of angles, the average divergence for each implant position significantly favored SPG, recording 0.38° (± 0.29) as opposed to IOS's 0.79° (± 0.59). It is essential to thoroughly interpret the clinical significance of this 0.40° angular disparity, considering the total number of implants within each complete arch. Furthermore, the significant deviations between the two evaluated devices for each implant position reached as high as 2.7486° in favor of SPG. Such discrepancies strongly indicate the potential superiority of SPG as a more dependable alternative to IOS for complete-arch digital implant impressions.

Although it is still advisable to conduct a rigid prototype try-in prior to manufacturing definitive screw-retained complete prostheses, recent findings from an in vivo study showcased similar results for two distinct IOS and SPG systems. However, the clinical performance of these systems was not assessed and compared within the same patient [15]. SPG demonstrated higher accuracy compared to IOS, with discrepancies ranging from 2.70 μm to 92.80 μm and a median of 17.00

μm, in contrast to IOS ranging from 21.30 μm to 815.60 μm and a median of 48.95 μm. Furthermore, SPG's accuracy remained unaffected by implant position or quantity. The passive fits of prosthetic frameworks produced by SPG and laboratory scanning were found to be comparable. Another in vivo study scrutinized the precision of two IOS devices and one SPG device in both arches of a single patient. Among these, SPG exhibited the highest repeatability concerning interimplant distance and angular deviation. The accuracy of SPG remained consistent regardless of arch type, whereas IOS devices demonstrated inferior performance in the mandible [71]. Within the context of the present study, SPG exhibited lower standard deviations across linear, 3D, and angular deviations in comparison to IOS.

The average 3D and angular values reported by IOS may potentially have an adverse impact on the overall fit between implants and prostheses, in contrast to SPG, which demonstrated notably superior performance in terms of 3D and angular deviations. As a result, the clinical utilization of SPG for complete-arch digital impressions is more advisable and practical. It is important to note that the deviations reported solely pertain to the impression process and do not encompass errors originating from other essential stages involved in crafting an implant-supported prosthesis. However, both systems revealed substantial deviations that exceeded the clinically acceptable threshold values (IOS: 558.1 μm [ΔEUC] and 2.89° [ΔANGLE]; SPG: 316.2 μm and 1.92°). Consequently, the implementation of SPG in routine clinical practice should be approached cautiously, emphasizing the necessity for a rigorous prototype try-in before finalizing the production of screw-retained complete-arch prostheses. Additional clinical investigations are imperative to gather precise data from a larger sample size, particularly regarding the influence of arch type and the number of implants on ΔEUC. Furthermore, it is essential to explore the effects of other production stages to validate the assessed technologies and the associated CAD-CAM workflow in the production of screw-retained zirconia-based complete-arch fixed dental prostheses.

The primary limitation of our clinical study lies in the intrinsic nature of the outcomes reported, which are specific to the investigated Intraoral Scanning (IOS) and Scanning Pattern Generator (SPG) systems. It is advisable to exercise prudence when extrapolating these findings to alternative devices. Nonetheless, it is noteworthy that the study examined one of the commercially accessible SPG devices and one of the extensively studied IOS systems, well-represented in the scientific literature. Additionally, the consistent execution of all scans by a singular expert clinician might have potentially masked certain distinctions between the systems attributable to variations in operator proficiency and expertise, which could warrant further investigation.

VI. CONCLUSIONS

Through the studies covered in this thesis, we have demonstrated the following novel scientific findings, which are directly related to the work that has been accomplished. It was found that:

1. Stereophotogrammetry (SPG) exhibited significantly higher 3D and angular accuracies compared to intra-oral scanners (IOS) both *in vitro* and *in vivo*.
2. SPG outperformed IOS with higher precision, reduced deviations, and consistent performance both *in vitro* and *in vivo*.
3. SPG displayed consistent measurement repeatability in both settings both *in vitro* and *in vivo*.
4. IOS exhibited extreme deviations exceeding clinically acceptable thresholds both *in vitro* and *in vivo*.
5. *In vivo*, the type of arch (i.e., mandible or maxilla) or the number of implants (4 or 6) did not have a significant effect on the outcomes, regardless of whether SPG or IOS was used for the digital impressions.

Based on these findings, we conclude that stereophotogrammetry appears to be more feasible than IOS for complete arch digital implant impressions, as the reported IOS deviations may negatively affect the overall implant-prosthesis fit, particularly in screw-retained complete-arch restorations. Nonetheless, its clinical implementation demands careful consideration, with emphasis on the prudent execution of a rigid prototype try-in before proceeding to manufacture definitive screw-retained complete-arch prostheses.

VII. ACKNOWLEDGEMENTS

To my lovely Mum, Anna, for her endless love and support throughout my life. To my brother, Giuseppe, who inspired and motivated my personal and professional growth. To my beloved wife, Camilla, thank you for your unconditional love, and for understanding all the time that I've been spending far from each other and our kids to conduct my research, pursue my passion for high-end dentistry, and train colleagues in advanced technologies to raise the level of care for our patients. Finally, I want to acknowledge Professor Katalin Nagy and Dr. Gábor Braunitzer for their wise guidance in all the stages of this PhD academic journey.

References

1. Sanda M, Miyoshi K, Baba K. Trueness and precision of digital implant impressions by intraoral scanners: a literature review. *Int J Implant Dent* 2021;7(1):97.

2. Arcuri L, Pozzi A, Lio F, Rompen E, Zechner W, Nardi A. Influence of implant scanbody material, position and operator on the accuracy of digital impression for complete-arch: A randomized in vitro trial. *J Prosthodont Res* 2020;64(2):128-36.

3. Rungruanganunt P, Taylor T, Eckert SE, Karl M. The effect of static load on dental implant survival: a systematic review. *Int J Oral Maxillofac Implants* 2013;28(5):1218-25.

4. Jemt T, Lie A. Accuracy of implant-supported prostheses in the edentulous jaw: analysis of precision of fit between cast gold-alloy frameworks and master casts by means of a three-dimensional photogrammetric technique. *Clin Oral Implants Res* 1995;6(3):172-80.

5. Pozzi A, Arcuri L, Lio F, Papa A, Nardi A, Londono J. Accuracy of complete-arch digital implant impression with or without scanbody splinting: An in vitro study. *J Dent* 2022;119:104072.

6. Pradies G, Ferreiroa A, Ozcan M, Gimenez B, Martinez-Rus F. Using stereophotogrammetric technology for obtaining intraoral digital impressions of implants. *J Am Dent Assoc* 2014;145(4):338-44.

7. Katsoulis J, Takeichi T, Sol Gaviria A, Peter L, Katsoulis K. Misfit of implant prostheses and its impact on clinical outcomes. Definition, assessment and a systematic review of the literature. *Eur J Oral Implantol* 2017;10 Suppl 1:121-38.

8. Nascimento C, Ikeda LN, Pita MS, Pedroso e Silva RC, Pedrazzi V, Albuquerque RF, et al. Marginal fit and microbial leakage along the implant-abutment interface of fixed partial prostheses: An in vitro analysis using Checkerboard DNA-DNA hybridization. *J Prosthet Dent* 2015;114(6):831-8.

9. Dias EC, Bisognin ED, Harari ND, Machado SJ, da Silva CP, Soares GD, et al. Evaluation of implant-abutment microgap and bacterial leakage in five external-hex implant systems: an in vitro study. *Int J Oral Maxillofac Implants* 2012;27(2):346-51.

10. Aglietta M, Siciliano VI, Zwahlen M, Bragger U, Pjetursson BE, Lang NP, et al. A systematic review of the survival and complication rates of implant supported fixed dental prostheses with cantilever extensions after an observation period of at least 5 years. *Clin Oral Implants Res* 2009;20(5):441-51.

11. Pozzi A, Tallarico M, Mangani F, Barlattani A. Different implant impression techniques for edentulous patients treated with CAD/CAM complete-arch prostheses: a randomised controlled trial reporting data at 3 year post-loading. *Eur J Oral Implantol* 2013;6(4):325-40.

12. Gomez-Polo M, Sallorenzo A, Cascos R, Ballesteros J, Barmak AB, Revilla-Leon M. Conventional and digital complete-arch implant impression techniques: An in vitro study comparing accuracy. *J Prosthet Dent* 2022.

13. Ahlholm P, Sipila K, Vallittu P, Jakonen M, Kotiranta U. Digital Versus Conventional Impressions in Fixed Prosthodontics: A Review. *J Prosthodont* 2018;27(1):35-41.

14. Nandini VV, Venkatesh KV, Nair KC. Alginate impressions: A practical perspective. *J Conserv Dent* 2008;11(1):37-41.

15. Yan Y, Lin X, Yue X, Geng W. Accuracy of 2 direct digital scanning techniques-intraoral scanning and stereophotogrammetry-for complete arch implant-supported fixed prostheses: A prospective study. *J Prosthet Dent* 2022.

16. Mangano A, Beretta M, Luongo G, Mangano C, Mangano F. Conventional Vs Digital Impressions: Acceptability, Treatment Comfort and Stress Among Young Orthodontic Patients. *Open Dent J* 2018;12:118-24.

17. Sivaramakrishnan G, Alsobaiei M, Sridharan K. Patient preference and operating time for digital versus conventional impressions: a network meta-analysis. *Aust Dent J* 2020;65(1):58-69.

18. Amin S, Weber HP, Finkelman M, El Rafie K, Kudara Y, Papaspyridakos P. Digital vs. conventional full-arch implant impressions: a comparative study. *Clin Oral Implants Res* 2017;28(11):1360-7.

19. Rutkunas V, Geciauskaite A, Jegelevicius D, Vaitiekunas M. Accuracy of digital implant impressions with intraoral scanners. A systematic review. *Eur J Oral Implantol* 2017;10 Suppl 1:101-20.

20. Rutkunas V, Gedrimiene A, Akulauskas M, Fehmer V, Sailer I, Jegelevicius D. In vitro and in vivo accuracy of full-arch digital implant impressions. *Clin Oral Implants Res* 2021;32(12):1444-54.

21. Mangano F, Gandolfi A, Luongo G, Logozzo S. Intraoral scanners in dentistry: a review of the current literature. *BMC Oral Health* 2017;17(1):149.

22. Angelone F, Ponsiglione AM, Ricciardi C, Cesarelli G, Sansone M, Amato F. Diagnostic Applications of Intraoral Scanners: A Systematic Review. *J Imaging* 2023;9(7).

23. Christopoulou I, Kaklamanos EG, Makrygiannakis MA, Bitsanis I, Perlea P, Tsolakis AI. Intraoral Scanners in Orthodontics: A Critical Review. *Int J Environ Res Public Health* 2022;19(3).

24. Amornvit P, Rokaya D, Sanohkan S. Comparison of Accuracy of Current Ten Intraoral Scanners. *Biomed Res Int* 2021;2021:2673040.

25. Abduo J, Elseyoufi M. Accuracy of Intraoral Scanners: A Systematic Review of Influencing Factors. *Eur J Prosthodont Restor Dent* 2018;26(3):101-21.

26. Kihara H, Hatakeyama W, Komine F, Takafuji K, Takahashi T, Yokota J, et al. Accuracy and practicality of intraoral scanner in dentistry: A literature review. *J Prosthodont Res* 2020;64(2):109-13.

27. Sacher M, Schulz G, Deyhle H, Jager K, Muller B. Accuracy of commercial intraoral scanners. *J Med Imaging (Bellingham)* 2021;8(3):035501.

28. Chiu A, Chen YW, Hayashi J, Sadr A. Accuracy of CAD/CAM Digital Impressions with Different Intraoral Scanner Parameters. *Sensors (Basel)* 2020;20(4).

29. Siqueira R, Galli M, Chen Z, Mendonca G, Meirelles L, Wang HL, et al. Intraoral scanning reduces procedure time and improves patient comfort in fixed prosthodontics and implant dentistry: a systematic review. *Clin Oral Investig* 2021;25(12):6517-31.

30. Christopoulou I, Kaklamanos EG, Makrygiannakis MA, Bitsanis I, Tsolakis AI. Patient-reported experiences and preferences with intraoral scanners: a systematic review. *Eur J Orthod* 2022;44(1):56-65.

31. Serrano-Velasco D, Martin-Vacas A, Paz-Cortes MM, Giovannini G, Cintora-Lopez P, Aragoneses JM. Intraoral scanners in children: evaluation of the patient perception, reliability and reproducibility, and chairside time-A systematic review. *Front Pediatr* 2023;11:1213072.

32. Yuzbasioglu E, Kurt H, Turunc R, Bilir H. Comparison of digital and conventional impression techniques: evaluation of patients' perception, treatment comfort, effectiveness and clinical outcomes. *BMC Oral Health* 2014;14:10.

33. Bosoni C, Nieri M, Franceschi D, Souki BQ, Franchi L, Giuntini V. Comparison between digital and conventional impression techniques in children on preference, time and comfort: A crossover randomized controlled trial. *Orthod Craniofac Res* 2023.

34. Burhardt L, Livas C, Kerdijk W, van der Meer WJ, Ren Y. Treatment comfort, time perception, and preference for conventional and digital impression techniques: A comparative study in young patients. *Am J Orthod Dentofacial Orthop* 2016;150(2):261-7.

35. Patzelt SB, Lamprinos C, Stampf S, Att W. The time efficiency of intraoral scanners: an in vitro comparative study. *J Am Dent Assoc* 2014;145(6):542-51.

36. Pozzi A, Gargari M, Barlattani A. CAD/CAM technologies in the surgical and prosthetic treatment of the edentulous patient with biomymetic individualized approach. *Oral Implantol (Rome)* 2008;1(1):2-14.

37. Guzzo F, G DEL, Barnaba P, Severino D. Cad-cam procedure and implant-prosthetic rehaBilitation. Case report. *Oral Implantol (Rome)* 2016;9(1):27-32.

38. Imburgia M, Logozzo S, Hauschild U, Veronesi G, Mangano C, Mangano FG. Accuracy of four intraoral scanners in oral implantology: a comparative in vitro study. *BMC Oral Health* 2017;17(1):92.

39. Revilla-Leon M, Att W, Ozcan M, Rubenstein J. Comparison of conventional, photogrammetry, and intraoral scanning accuracy of complete-arch implant impression procedures evaluated with a coordinate measuring machine. *J Prosthet Dent* 2021;125(3):470-8.

40. Revilla-Leon M, Kois DE, Kois JC. A guide for maximizing the accuracy of intraoral digital scans: Part 2-Patient factors. *J Esthet Restor Dent* 2023;35(1):241-9.

41. Revilla-Leon M, Kois DE, Kois JC. A guide for maximizing the accuracy of intraoral digital scans. Part 1: Operator factors. *J Esthet Restor Dent* 2023;35(1):230-40.

42. Gomez-Polo M, Immorlano MG, Cascos-Sanchez R, Ortega R, Barmak AB, Kois JC, et al. Influence of the dental arch and number of cutting-off and rescanning mesh holes on the accuracy of implant scans in partially edentulous situations. *J Dent* 2023:104667.

43. Gomez-Polo M, Piedra-Cascon W, Methani MM, Quesada-Olmo N, Farjas-Abadia M, Revilla-Leon M. Influence of rescanning mesh holes and stitching procedures on the complete-arch scanning accuracy of an intraoral scanner: An in vitro study. *J Dent* 2021;110:103690.

44. Revilla-Leon M, Quesada-Olmo N, Gomez-Polo M, Sicilia E, Farjas-Abadia M, Kois JC. Influence of rescanning mesh holes on the accuracy of an intraoral scanner: An in vivo study. *J Dent* 2021;115:103851.

45. Huang R, Liu Y, Huang B, Zhang C, Chen Z, Li Z. Improved scanning accuracy with newly designed scan bodies: An in vitro study comparing digital versus conventional impression techniques for complete-arch implant rehabilitation. *Clin Oral Implants Res* 2020;31(7):625-33.

46. Imburgia M, Kois J, Marino E, Lerner H, Mangano FG. Continuous Scan Strategy (CSS): A Novel Technique to Improve the Accuracy of Intraoral Digital Impressions. *Eur J Prosthodont Restor Dent* 2020;28(3):128-41.

47. Gomez-Polo M, Gomez-Polo C, Del Rio J, Ortega R. Stereophotogrammetric impression making for polyoxymethylene, milled immediate partial fixed dental prostheses. *J Prosthet Dent* 2018;119(4):506-10.

48. Lie A, Jemt T. Photogrammetric measurements of implant positions. Description of a technique to determine the fit between implants and superstructures. *Clin Oral Implants Res* 1994;5(1):30-6.

49. Pozzi A, Arcuri L, Carosi P, Nardi A, Kan J. Clinical and radiological outcomes of novel digital workflow and dynamic navigation for single-implant immediate loading in aesthetic zone: 1-year prospective case series. *Clin Oral Implants Res* 2021;32(12):1397-410.

50. Agustin-Panadero R, Penarrocha-Oltra D, Gomar-Vercher S, Penarrocha-Diago M. Stereophotogrammetry for Recording the Position of Multiple Implants: Technical Description. *Int J Prosthodont* 2015;28(6):631-6.

51. Penarrocha-Diago M, Balaguer-Marti JC, Penarrocha-Oltra D, Balaguer-Martinez JF, Penarrocha-Diago M, Agustin-Panadero R. A combined digital and stereophotogrammetric technique for rehabilitation with immediate loading of complete-arch, implant-supported prostheses: A randomized controlled pilot clinical trial. *J Prosthet Dent* 2017;118(5):596-603.

52. Kottner S, Schaerli S, Furst M, Ptacek W, Thali M, Gascho D. VirtoScan-on-Rails - an automated 3D imaging system for fast post-mortem whole-body surface documentation at autopsy tables. *Forensic Sci Med Pathol* 2019;15(2):198-212.

53. Peake M, Pan K, Rotatori RM, Powell H, Fowler L, James L, et al. Incorporation of 3D stereophotogrammetry as a reliable method for assessing scar volume in standard clinical practice. *Burns* 2019;45(7):1614-20.

54. Heike CL, Upson K, Stuhaug E, Weinberg SM. 3D digital stereophotogrammetry: a practical guide to facial image acquisition. *Head Face Med* 2010;6:18.

55. Dindaroglu F, Kutlu P, Duran GS, Gorgulu S, Aslan E. Accuracy and reliability of 3D stereophotogrammetry: A comparison to direct anthropometry and 2D photogrammetry. *Angle Orthod* 2016;86(3):487-94.

56. Peñarrocha-Oltra D, Agustín-Panadero R, Bagán L, Giménez B, Peñarrocha M. Impression of multiple implants using photogrammetry: description of technique and case presentation. *Med Oral Patol Oral Cir Bucal* 2014;19(4):e366-71.

57. Ma B, Yue X, Sun Y, Peng L, Geng W. Accuracy of photogrammetry, intraoral scanning, and conventional impression techniques for complete-arch implant rehabilitation: an in vitro comparative study. *BMC Oral Health* 2021;21(1):636.

58. Revilla-Leon M, Rubenstein J, Methani MM, Piedra-Cascon W, Ozcan M, Att W. Trueness and precision of complete-arch photogrammetry implant scanning assessed with a coordinate-measuring machine. *J Prosthet Dent* 2023;129(1):160-5.

59. Muller P, Ender A, Joda T, Katsoulis J. Impact of digital intraoral scan strategies on the impression accuracy using the TRIOS Pod scanner. *Quintessence Int* 2016;47(4):343-9.

60. Johansson A, Omar R, Carlsson GE. Bruxism and prosthetic treatment: a critical review. *J Prosthodont Res* 2011;55(3):127-36.

61. Agliardi EL, Pozzi A, Stappert CF, Benzi R, Romeo D, Gherlone E. Immediate fixed rehabilitation of the edentulous maxilla: a prospective clinical and radiological study after 3 years of loading. *Clin Implant Dent Relat Res* 2014;16(2):292-302.

62. Agliardi EL, Pozzi A, Romeo D, Del Fabbro M. Clinical outcomes of full-arch immediate fixed prostheses supported by two axial and two tilted implants: A retrospective cohort study with 12-15 years of follow-up. *Clin Oral Implants Res* 2023;34(4):351-66.

63. Pozzi A, Arcuri L, M SB, P KM. Digital assisted soft tissue sculpturing (DASS) technique for immediate loading pink free complete arch implant prosthesis. *J Prosthodont Res* 2021;65(1):119-24.

64. Pozzi A, Hansson L, Carosi P, Arcuri L. Dynamic navigation guided surgery and prosthetics for immediate loading of complete-arch restoration. *J Esthet Restor Dent* 2021;33(1):224-36.

65. Abduo J, Lyons K, Swain M. Fit of zirconia fixed partial denture: a systematic review. *J Oral Rehabil* 2010;37(11):866-76.

66. Kan JY, Rungcharassaeng K, Bohsali K, Goodacre CJ, Lang BR. Clinical methods for evaluating implant framework fit. *J Prosthet Dent* 1999;81(1):7-13.

67. Mizumoto RM, Yilmaz B, McGlumphy EA, Jr., Seidt J, Johnston WM. Accuracy of different digital scanning techniques and scan bodies for complete-arch implant-supported prostheses. *J Prosthet Dent* 2020;123(1):96-104.

68. Tohme H, Lawand G, Chmielewska M, Makhzoume J. Comparison between stereophotogrammetric, digital, and conventional impression techniques in implant-supported fixed complete arch prostheses: An in vitro study. *J Prosthet Dent* 2023;129(2):354-62.

69. Schwarz MS. Mechanical complications of dental implants. *Clin Oral Implants Res* 2000;11 Suppl 1:156-8.

70. Pozzi A, Arcuri L, Fabbri G, Singer G, Londono J. Long-term survival and success of zirconia screw-retained implant-supported prostheses for up to 12 years: A retrospective multicenter study. *J Prosthet Dent* 2023;129(1):96-108.

71. Orejas-Perez J, Gimenez-Gonzalez B, Ortiz-Collado I, Thuissard IJ, Santamaria-Laorden A. In Vivo Complete-Arch Implant Digital Impressions: Comparison of the Precision of Three Optical Impression Systems. *Int J Environ Res Public Health* 2022;19(7).

72. Peroz S, Spies BC, Adali U, Beuer F, Wesemann C. Measured accuracy of intraoral scanners is highly dependent on methodical factors. *J Prosthodont Res* 2022;66(2):318-25.

73. Chochlidakis K, Papaspyridakos P, Tsigarida A, Romeo D, Chen YW, Natto Z, et al. Digital Versus Conventional Full-Arch Implant Impressions: A Prospective Study on 16 Edentulous Maxillae. *J Prosthodont* 2020;29(4):281-6.

74. Pesce P, Pera F, Setti P, Menini M. Precision and Accuracy of a Digital Impression Scanner in Full-Arch Implant Rehabilitation. *Int J Prosthodont* 2018;31(2):171-5.

75. Treesh JC, Liacouras PC, Taft RM, Brooks DI, Raiciulescu S, Ellert DO, et al. Complete-arch accuracy of intraoral scanners. *J Prosthet Dent* 2018;120(3):382-8.

76. Abduo J. Fit of CAD/CAM implant frameworks: a comprehensive review. *J Oral Implantol* 2014;40(6):758-66.

77. Mericske-Stern R, Worni A. Optimal number of oral implants for fixed reconstructions: a review of the literature. *Eur J Oral Implantol* 2014;7 Suppl 2:S133-53.

78. Manzella C, Bignardi C, Burello V, Carossa S, Schierano G. Method to improve passive fit of frameworks on implant-supported prostheses: An in vitro study. *J Prosthet Dent* 2016;116(1):52-8.

79. de Franca DG, Morais MH, das Neves FD, Carreiro AF, Barbosa GA. Precision Fit of Screw-Retained Implant-Supported Fixed Dental Prostheses Fabricated by CAD/CAM, Copy-Milling, and Conventional Methods. *Int J Oral Maxillofac Implants* 2017;32(3):507-13.

80. Ortorp A, Jemt T, Back T, Jalevik T. Comparisons of precision of fit between cast and CNC-milled titanium implant frameworks for the edentulous mandible. *Int J Prosthodont* 2003;16(2):194-200.

APPENDIX

J Prosthodont Res. 2023; **(**): ****–****

OPEN ACCESS JPR Journal of Prosthodontic Research Original article

Accuracy of intraoral optical scan versus stereophotogrammetry for complete-arch digital implant impression: An *in vitro* study

Alessandro Pozzi [a,b], Enrico Agliardi [c], Fabrizio Lio [d], Katalin Nagy [e], Alessandra Nardi [f], Lorenzo Arcuri [g,*]

[a] Goldstein Center for Esthetic and Implant Dentistry, Department of Restorative Sciences, Augusta University, Augusta, USA, [b] Department of Clinical Sciences and Translational Medicine, School of Dentistry, University of Tor Vergata, Rome, Italy, [c] Dentistry Department, Vita e Salute San Raffaele University, Milan, Italy, [d] Department of Chemical Science and Technologies, Materials for Health, Environment and Energy - Dentistry, University of Tor Vergata, Rome, Italy, [e] Department of Oral Surgery, University of Szeged, Hungary, [f] Department of Mathematics, University of Rome Tor Vergata, Rome, Italy, [g] Department of Odontostomatological and Maxillofacial Sciences, Sapienza University, Rome, Italy

Abstract

Purpose: To assess and compare the accuracies of intraoral scanners (IOS) and stereophotogrammetry (SPG) devices for complete-arch digital implant impressions.

Methods: A 4-analog model was digitized using a desk scanner to obtain a reference file. Thirty test scans were conducted using the investigated IOS device, while an additional 30 scans were performed using the SPG device. Using the best-fit algorithm, the resulting 60 test files were aligned with the reference file. Linear (ΔX, ΔY, and ΔZ-axis) and angular deviations (ΔANGLE) were evaluated. Three-dimensional (3D) deviation was calculated based on the Euclidean distance (ΔEUC). The analysis was stratified according to the scanning device and implant position. Fisher's F and t-tests were used to compare the variances and expected values of the two scanning systems.

Results: IOS expressed a higher 3D (ΔEUC) mean deviation than SPG (52.8 μm vs. 33.4 μm, $P < 0.0001$), with extreme measurements up to 181.9 μm. A significantly higher standard deviation (SD) was associated with IOS (37.1 μm vs. 17.7 μm, $P < 0.0001$). Considering angular deviations, the IOS showed slightly higher angular mean deviations (ΔANGLE) than the SPG (0.28° vs. 0.24°, $P = 0.0022$), with extreme measurements of up to 0.73°. The SPG SD values were significantly lower than the IOS SD values (0.14° vs. 0.04°, $P < 0.0001$).

Conclusions: The SPG showed significantly higher 3D and angular accuracies for complete arch implant impressions, with consistent repeatability. IOS scanning revealed significantly higher extreme deviations exceeding the acceptable threshold value. Despite study limitations, SPG appears more feasible than IOS for complete-arch digital implant impressions.

Keywords: Intraoral scanner, Stereophotogrammetry, Complete arch, Digital impression

Received 2 October 2022, Accepted 19 July 2023, Available online 11 August 2023

1. Introduction

Digital impressions are considered a valid alternative to conventional impressions for recording the intraoral anatomy and implant positions[1,2]. Since the introduction of the first digital intraoral scanner (IOS) in the 1980s, several devices based on different optical technologies, such as confocal microscopy, optical coherence tomography, active and passive stereovision and triangulation, interferometry, and phase shift principles, have been proposed[3]. Initially, the use of a coating powder was necessary to allow proper surface scanning, minimize noise, and increase the practicality[3]. Currently, the improvement of intraoral optical surface scanning technology has broadened the clinical use of digital impression techniques, which are becoming essential in modern dentistry. The IOS allows for increased operative comfort, particularly in patients with a pronounced gag reflex, and transfers the patient dataset to all dental team members, enhancing the comprehensive diagnosis, treatment plan, and patient monitoring over the years. Moreover, digital impressions eliminate errors related to impressions, pouring materials, and casting laboratory procedures[4].

Furthermore, digital impressions enhance computer-aided design and computer-aided manufacturing (CAD-CAM) production processes that enable the use of esthetic milling materials, such as zirconia and alumina, and the use of three-dimensional (3D) printing materials that cannot be cast or produced in an analogical conventional manner[4].

The IOS accuracy is reliable for digital impressions of single crowns and short-span fixed dental prostheses[5]. However, IOS accuracy is influenced by different operators (scanning technology and system selection, scanning head size, calibration, scanning distance, exposure of the IOS to ambient temperature changes, ambient humidity, ambient lighting conditions, operator experience, scanning

DOI: https://doi.org/10.2186/jpr.JPR_D_22_00251
***Corresponding author:** Lorenzo Arcuri, Department of Odontostomatological and Maxillofacial Sciences, Sapienza University, 00161 Rome.
E-mail address: lorenzo.arcuri@uniroma1.it

pattern, extension of the scan, cutting off, rescanning, and overlapping) and patient factors (tooth type, presence of interdental spaces, arch width variations, palate characteristics, wetness, existing restorations, characteristics of the surface being digitized, edentulous areas, inter-implant distance, position, angulation, depth of existing implants, and implant scanbody (ISB) selection)[6,7]. Accuracy is defined by trueness and precision (ISO5725-1). Trueness describes the conformity of measurements to actual values, and precision describes the conformity of multiple repeated measurements[8]. The IOS for complete arch implant impressions remains controversial by the dental community in terms of accuracy and practicality, particularly for the lower jaw[9,10]. A recent literature review on IOS accuracy and practicality showed that the longer the scan range, the larger the error, with trueness below 50 µm and between 50 and 250 µm for partial and complete arch digital impressions, respectively[6].

This issue is intrinsic to the IOS 3D reconstruction algorithm, which is based on the stitching imaging process. The 3D images consecutively acquired by the IOS device must be stitched using the IOS software algorithm during the scanning procedure, using reference stable points represented by teeth, gingiva, or other anatomical structures. Therefore, a scanning strategy featuring slow-speed buccolingual wave movement is mandatory to facilitate consecutive image acquisition and 3D reconstruction[4,11].

Long-span edentulous ridges and completely edentulous arches represent difficult clinical scenarios for IOS because of the lack of stable and easy-to-identify anatomical reference points. The use of artificial reference points such as adhesive landmarks, temporary anchorage device (TAD) screws, or splinting systems has been advocated to facilitate image acquisition and 3D anatomic scanning of edentulous patients, although their clinical application can be cumbersome[11].

Stereophotogrammetry (SPG) was first proposed by Lie and Jemt as a method for determining the misfit between implants and frameworks[12,13]. In 1999, Jemt *et al.* reported that this technology is a suitable substitute for conventional impressions of complete arches[14].

SPG is a digital impression technology that detects only implant coordinates, whereas intraoral dental and gingival anatomies cannot be detected[15]. SPG is based on an extraoral device with two cameras that simultaneously detect a specific optical landmark geometry featuring the surface of dedicated flag ISBs[16]. No stitching process is considered in the SPG technology[14]. The extraoral scan and different detection methods of implant coordinates without the stitching process algorithm suggest a potential clinical application of SPG as a digital alternative to IOS for complete arch implant impressions.

Studies comparing the *in vitro* accuracy of IOS and SPG for complete arch implant digital impressions are already available in the scientific literature, although conflicting results have been reported[10,17,18]. The paucity of current scientific evidence on the topic requires further investigations with larger sample sizes and powerful statistics to achieve a more detailed conclusion on the accuracy of these digital impression technologies. This *in vitro* study aimed to assess and compare the accuracy of IOS and SPG for complete arch implant impressions in a mandibular model fitted with four implant analogs. The null hypothesis was that there would be no significant differences in 3D and angular deviations between the investigated complete-arch digital implant impression techniques.

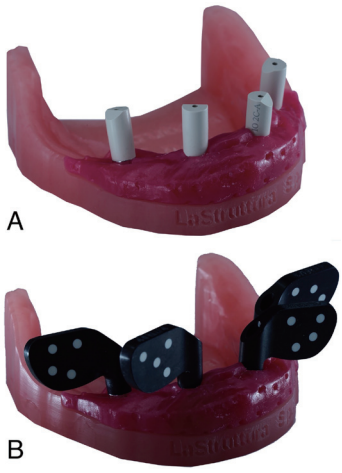

Fig. 1. A. Mandibular polymethylmethacrylate (PMMA) model with removable soft tissue frame and polyether ether ketone (PEEK) ISBs screwed onto the MUA implant analogs. B. Mandibular PMMA model with removable soft tissue frame and 4 stereophotogrammetry scanbodies screwed onto the MUA implant analogs.

2. Materials and Methods

2.1. Master model

An edentulous mandibular polymethylmethacrylate (PMMA) milled model with four multiunit implant analogs (MUA analogs; Nobel Biocare, Kloten, Switzerland) positioned at 3.2, 3.5, 4.2 and 4.5 was produced. The following implant position criteria were adopted: 3.2 (depth -1 mm, distal angulation 5°), 3.5 (depth -3 mm, mesial angulation 10°), 4.2 (depth 0 mm, angulation 0°), and 4.5 (depth -4 mm, distal angulation 15°). A removable soft tissue frame was 3D printed (NextDent 5100, 3DSystems, Rock Hill, SC, USA) with a dedicated material (Gingiva Mask, NextDent, 3DSystems, Rock Hill, SC, USA) to ensure the fit of the scan bodies on the model and to provide the opportunity to check the fit.

2.2. Reference scan

A four-Blue LED 5 MPa camera, scanner (D2000, 3 shape, Copenhagen, Denmark), properly calibrated before scanning, was used to obtain a standard tesselation language (STL) file to be used as reference. The scanner is certified for an accuracy of 5 µm, as specified in the ISO 12836 certification.

2.3. IOS and SPG scan procedures

One experienced operator who used both scanning devices and blinded to the study aims, was enrolled. A second operator secured the polyether ether ketone (PEEK) ISBs onto the MUA implant analogs with a 10 Ncm torque controlled by a dynamometer, and visually checked the proper ISB seating over the analog heads with magnifying loupes (Eyezoom 5X, Orascoptic, Middleton, WI, USA) (**Fig. 1A**). Thereafter, the second operator screwed the SPG scan bodies onto the MUA implant analogs using the same procedure (**Fig. 1B**). A total of 60 complete arch scans (30 scans for each device) were performed.

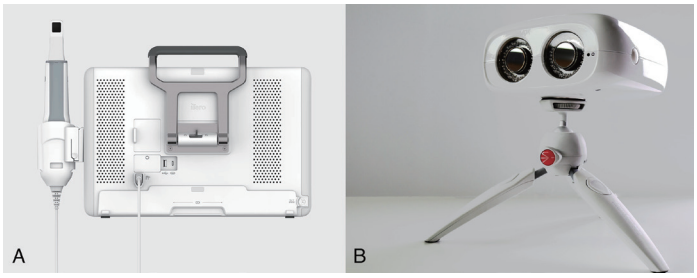

Fig. 2. A. Intraoral scanner device. B. Stereophotogrammetry device.

2.3.1. IOS scan procedure

The investigated IOS device was a pen grip (iTero Element 5D; Align Technology, Tempe, AZ, USA) (**Fig. 2A**). It is a powder-free scanner based on parallel confocal imaging laser technology. The IOS scans were acquired with a rest time of at least 5 min between the scans. The scan starting point was always the ISB at position 4.5, while 3.5 was the last one to be scanned. Before starting the investigation, the IOS calibration was performed by the producer.

The scan strategy was consistent for all scanning procedures according to the manufacturer's guidelines. The starting point for occlusal-lingual surface of the ISB was position 4.5, then it moved toward ISB 3.5, always including two surfaces, and returned from the buccal side[19].

2.3.2. SPG scan procedure

A SPG system (Precise Implant Capture, PiC camera, PiC Dental, Madrid, Spain) was used to record the implant positions (**Fig. 2B**). SPG ISBs were screwed onto multiunit abutments and their specific SPG codes were reported in the software for each implant site. The SPG camera was positioned 15–30 cm from the model at a 45° angulation. The images captured by the SPG device were processed using the SPG software to obtain the 3D coordinates of each implant in a vector format. Subsequently, STL files were exported.

2.4. Data processing and accuracy assessment

The 60 test STL files were aligned to the reference scan with dedicated software (Geomagic Studio 12, 3DSystems, Rock Hill, SC, USA) according to a 0.01 mm alignment tolerance, and two alignment optimizations were accomplished after file superimposition. Superimposition between the test and control group scans and the reference scan was obtained using the best-fit method, considering only the alignment of the implant positions and simulating a standard clinical and laboratory workflow.

The best-fit algorithm was used to measure the deviation of each implant from its analog in the reference file. Therefore, it was possible to properly analyze the 3D linear and angular deviations of each implant by considering the error distribution in the three spatial coordinates. Finally, the linear (ΔX, ΔY, and ΔZ) and angular discrepancies (ΔANGLE) between each test scan and the reference scan were measured for any analog, and the superimposed files were analyzed using dedicated measurement software (Hyper Cad S, Cam HyperMill, Open Mind Technologies, Milano, Italy) after reconstruction of the linear geometries of the analogs. The centers of the digital-analog heads were used for deviation measurements. Negative values on the X-, Y-, and Z-axes indicated an ISB positioned to the left, downward, and backward, respectively, whereas positive values were in the opposite direction on each axis. 3D deviations were calculated considering the Euclidean distance between the centers of the heads of the test and control implant analogs (ΔEUC) (**Figs. 3 and 4**)[9,11].

2.5. Statistical analysis

Assuming Euclidean distance as the primary endpoint and a significance level of 0.05, a sample size of 240 implants guaranteed a minimum expected difference of 20 μm and a test power of 0.95.

However, the sample size calculation was performed assuming an expected standard deviation of 40 μm for both IOS and SPG. Although this assumption was consistent with the observed standard deviation of the IOS, the observed SPG variability was significantly lower. Therefore, a post-hoc analysis based on the observed values was performed; assuming a test size of 0.05, the test power was 0.98.

Continuous variables are summarized as mean, standard deviation, and minimum and maximum values. Kernel density estimates were used to describe the empirical distributions. Fisher's F and t-tests were used to compare the variances and expected values between the two groups, respectively. Welch's t-test was used in cases with significantly different variances.

3. Results

Deviations between the reference scan and 60 test scans (30 IOS; 30 SPG) were calculated for each implant analog (n = 240) over the X-, Y-, and Z-axes and angulation. From the linear discrepancies, the 3D deviation was calculated in terms of the Euclidean distance (ΔEUC). The 3D and angular deviations did not consider the direction of the error. **Table 1** describes the deviations from the reference scans of the IOS and SPG.

IOS expressed higher 3D mean deviations (ΔEUC) compared to SPG (52.8 μm vs. 33.4 μm $P < 0.0001$) with extreme measurements up to 181.9 μm. Moreover, a significantly higher standard deviation (SD) was associated with IOS (37.1 μm vs. 17.7 μm $P < 0.0001$).

Considering angular deviations (ΔANGLE), IOS showed slightly higher mean deviations than SPG (0.28° vs. 0.24°, $P = 0.0022$), with extreme measurements of up to 0.73°. The SPG SD values were significantly lower than the IOS SD values (0.14 vs. 0.04°, $P < 0.0001$).

Tables 2 and 3 present the 3D and angular discrepancies stratified according to implant position and scanning device. The corresponding empirical distributions are shown in **Figures 5 and 6**.

Considering ΔEUC, implant site 4.5 was the most critical position to be scanned with the IOS (deviations up to 181.88 μm), while the anterior implants (4.2 and 3.2) were more critical for scanning with the SPG. The 3D variability was significantly reduced for SPG compared to IOS for all implants, except for implant 4.2, where the reduction in variability did not reach significance. No significant mean difference was observed between the two devices for implant 4.2 as well.

Figure 5 shows how IOS and SPG performed similarly for anterior implant 4.2; for posterior implants (4.5, 3.5), an evidently better

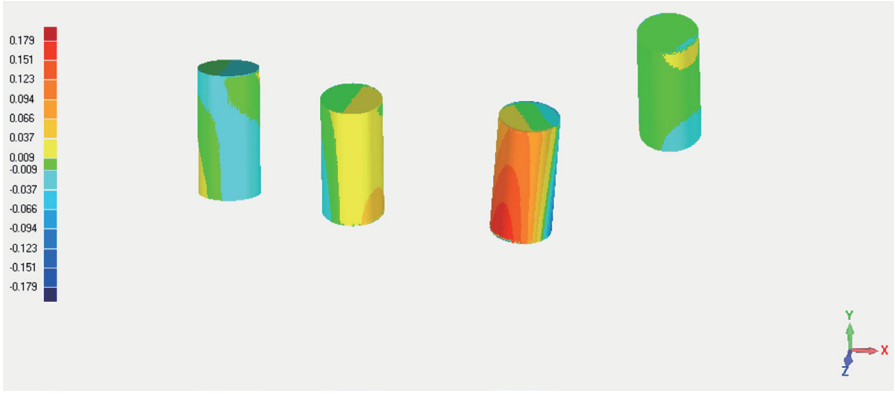

Fig. 3. Best fit algorithm alignment to superimpose the 4 implant positions of the test files with the corresponding positions of the reference file

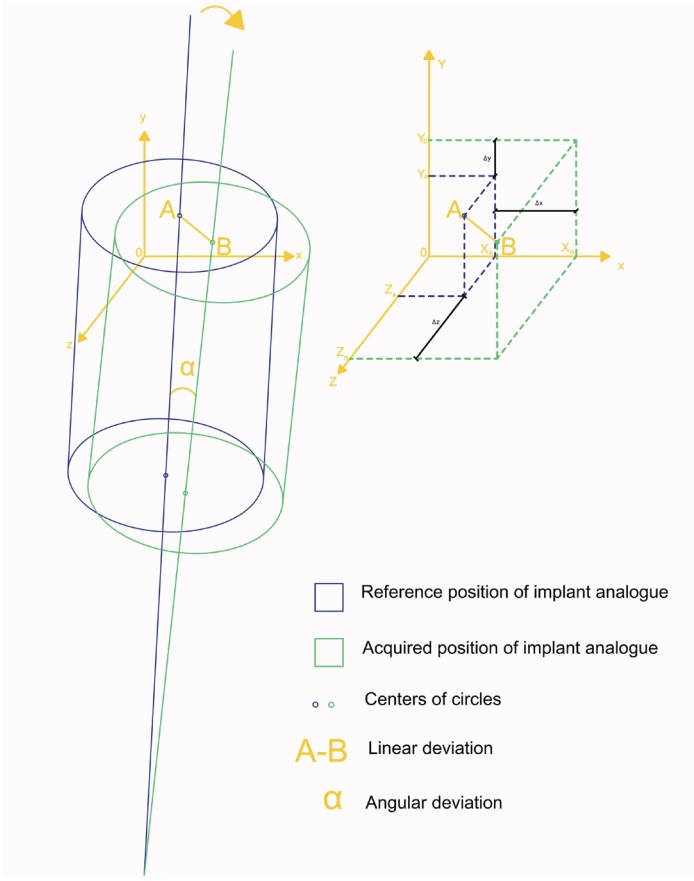

Fig. 4. 3D and angular deviation assessment. The 3D linear deviation (ΔEUC) was calculated as the distance between the head centers of the reference (A) and the corresponding reference of the acquired analog position (B). That distance was decomposed into the 3 space axes to calculate linear deviations (ΔX, ΔY, ΔZ). The angular deviation was calculated as the angle formed by the two lines passing orthogonally to the head of the analogs through Points A and B.

performance of SPG was detected, especially for implant 4.5.

Considering ΔANGLE, no significant differences were found in terms of implant position. The expected angular discrepancy was significantly different between the IOS and SPG only for implant 4.2 (0.40° vs. 0.23°, $P < 0.0001$). However, SPG always performed significantly better than IOS in terms of SD.

4. Discussion

This *in vitro* study analyzed and compared the accuracy of two digital impression methods (IOS and SPG) for complete arch implant impressions. The trueness and precision of IOS and SPG were compared as linear and angular deviations, respectively. The null hypothesis was rejected because the SPG performed better than the IOS in terms of both 3D (ΔEUC) trueness ($P < 0.0001$) and precision ($P < 0.0001$). Considering angular deviations (ΔANGLE), the SPG performed better than the IOS in terms of angular trueness ($P = 0.0022$) and precision ($P < 0.0001$). IOS expressed higher 3D mean deviations (ΔEUC) compared to SPG (52.8 µm vs. 33.4 µm $P < 0.0001$) with extreme measurements of up to 181.9 µm. A significantly higher SD was associated with IOS (37.1 µm vs. 17.7 µm $P < 0.0001$). Considering angular deviations (ΔANGLE), IOS showed slightly higher mean deviations than SPG (0.28° vs. 0.24°, $P = 0.0022$), with extreme measurements of up to 0.73°. The SPG SD values were significantly lower than the IOS SD values (0.14° vs. 0.04°, $P < 0.0001$).

The study design was based on the use of a best-fit alignment between the reference and test scans to measure the deviations for each implant position and further analyze the 3D deviation in each of the three space axes. The best-fit algorithm allows the deviation measurement of all implant positions by comparing the respective test and reference files. Thus, it was possible to properly analyze the deviations of each implant from a linear (ΔY, ΔX, ΔZ), 3D (ΔEUC) and angular (ΔANGLE) point of view. The Euclidean distance, as an index of 3D deviation, was preferred to the root mean square (RMS), as it is easier to translate as a metric outcome in clinical practice. The choice of a certified 5 µm accuracy optical desk scanner as a reference was justified by its better access to the freedom plane compared to tactile systems, such as the coordinate measuring machine (CMM)[20].

The study's limitations include being conducted in an *in vitro* environment, which may have underestimated deviations due to patient factors, such as saliva, blood, tongue, and movements[21]. However, the SPG extraoral scan offers a potential digital alternative to the IOS for complete-arch implant impressions, as it overcomes these limitations. In vivo studies are recommended to assess SPG's accuracy and practicality of SPG in challenging complete arch cases

Table 1. Descriptive analysis intraoral scanner (IOS) and stereophotogrammetry (SPG) linear, 3D and angular deviations

	IOS			SPG		
	Mean	Std. Deviation	Range	Mean	Std. Deviation	Range
ΔY (μm)	-2.03	14.54	(-71.86, 18.77)	0.95	7.15	(-13.09, 18.42)
ΔX (μm)	5.21	50.51	(-87.29, 146.55)	12.81	19.23	(-52.86, 51.67)
ΔZ (μm)	-1.85	37.31	(-117.53, 82.95)	20.78	20.42	(-43.16, 75.97)
ΔEUC (μm)	52.81	37.11	(4.18, 181.88)	33.42	17.71	(7.56, 80.34)
ΔANGLE (°)	0.28	0.14	(0.03, 0.73)	0.24	0.04	(0.15, 0.36)

Table 2. 3D distances (ΔEUC) stratified by implant and scanning device (μm). The F and t-tests were used to compare the variances and expected values between the two groups (intraoral scanner [IOS] and stereophotogrammetry [SPG]).

	IOS			SPG				
Implant	Mean	Std. Deviation	Range	Mean	Std. Deviation	Range	F test *P*-value	T test *P*-value
4.5	81.85	48.22	(15.72, 181.88)	29.25	3.73	(17.57, 35.41)	<0.0001	<0.0001*
4.2	43.46	22.43	(10.82, 81.59)	48.58	19.37	(15.36, 80.34)	0.4350	0.3474
3.2	56.14	27.17	(5.07, 103.18)	41.06	14.41	(22.54, 77.18)	0.0010	0.0102*
3.5	29.79	23.73	(4.18, 107.22)	14.78	3.83	(7.56, 22.51)	<0.0001	0.0018*

* *P*-value refers to Welch's t-test

Table 3. Angular discrepancies (ΔANGLE) stratified by implant and scanning device (°). The F-test and T test were used to compare the variances and expected values between the two groups (intraoral scanner [IOS] and stereophotogrammetry [SPG]).

	IOS			SPG				
Implant	Mean	Std. Deviation	Range	Mean	Std. Deviation	Range	F test *P*-value	T test *P*-value
4.5	0.29	0.13	(0.08, 0.73)	0.29	0.05	(0.19, 0.36)	<0.0001	0.8719*
4.2	0.40	0.13	(0.15, 0.67)	0.23	0.02	(0.20, 0.27)	<0.0001	<0.0001*
3.2	0.21	0.11	(0.03, 0.41)	0.24	0.02	(0.20, 0.29)	<0.0001	0.1820*
3.5	0.24	0.12	(0.09, 0.52)	0.21	0.03	(0.15, 0.26)	<0.0001	0.1728*

* *P*-value refers to Welch's t-test

with varying levels of bone and soft-tissue atrophy. The findings of this study are specific to the investigated IOS and SPG systems, and should be cautiously applied to other devices. While the scans were performed by a single expert clinician, previous research indicated no significant operator effect on the IOS accuracy[9]. Further research should explore the operator effect and learning curve of the SPG technology, as this information is currently lacking in the literature.

The study results were in line with the findings of a recent *in vitro* study by Thome *et al.*, who measured and compared the scan body coordinates of the reference cast with the scan body positions obtained using the conventional (impression plaster), IOS, and SPG techniques[17]. Thome *et al.* used the same SPG device as in the present study and a desk scanner with an accuracy of 7 μm as a reference. Moreover, the study analyzed the global angular distortion and 3D deviations of the entire scan body and flat-angled surface using an inspection and metrology software program and the best-fit alignment technique. Although the methods and IOS were different compared to those in the present study, the SPG technique reported the highest accuracy in terms of trueness and precision for the intraoral scan bodies of all the techniques evaluated.

Another *in vitro* study compared the accuracy of a conventional technique (elastomeric impression), SPG, and two IOSs using a CMM with a nominal linear accuracy of 1 μm as a reference and showed completely different results[10]. The SPG system (iCam4D; Imetric4D Imaging Sàrl, Courgenay, Switzerland) provided the least accurate values with the highest 3D discrepancy for implant positions among all groups, with a mean 3D deviation of 77.6 μm.

Another study compared the accuracy of conventional techniques (polyether impression) and SPG and IOS for complete-arch implant impressions using a 4 μm accuracy laboratory scanner as a reference[18]. The test and control files were superimposed using a best-fit algorithm, and the 3D discrepancy between the two STL files was evaluated using the RMS error calculated by the inspection software. The SPG obtained the lowest 3D discrepancy in terms of trueness and precision for the implant abutment positions, whereas the IOS showed the least accuracy among the three impression techniques tested. The two aforementioned studies investigated the same SPG system (iCam4D; Imetric4D Imaging Sàrl, Courgenay, Switzerland), although different reference systems (desk scanner) and analyzed measurements (RMS) were used. These differences in study designs justify the contradictory results reported. The authors reported a dramatically low mean 3D deviation of 33.4 ± 17.7 μm of the investigated SPG system (Precise Implant Capture, PiC camera, PiC dental, Madrid, Spain).

In the present study, IOS showed higher 3D mean deviations than SPG (52.8 μm vs. 33.4 μm $P < 0.0001$), with extreme measure-

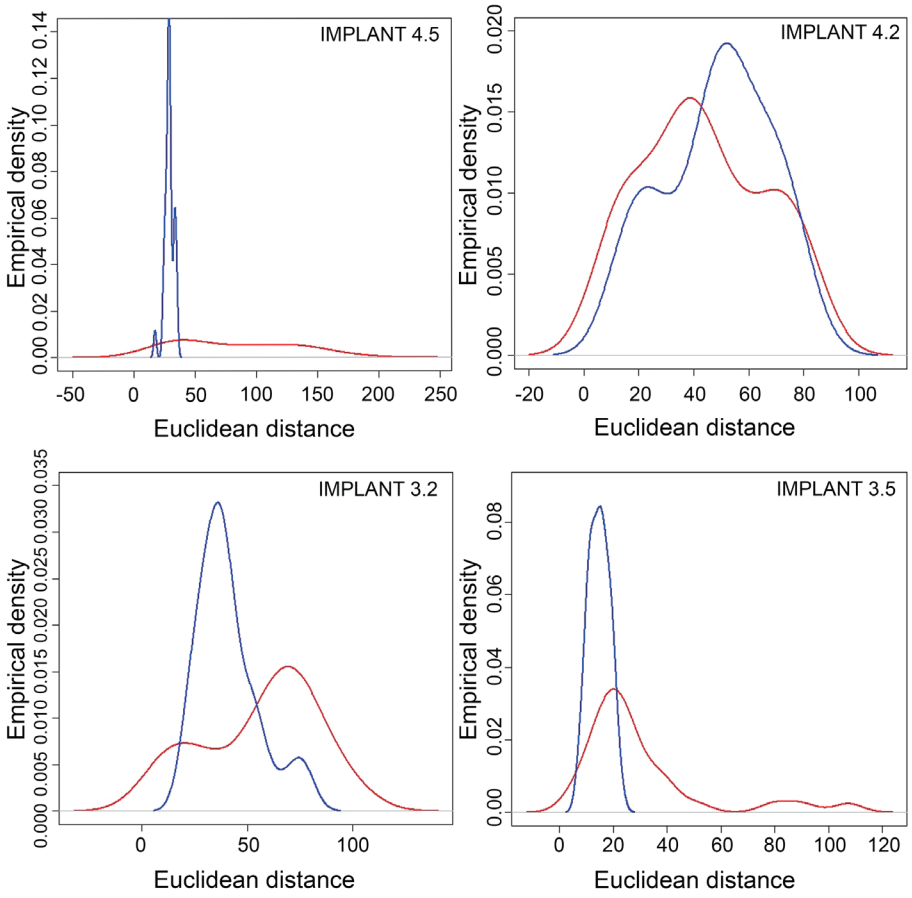

Fig. 5. Empirical distributions of 3D distances (ΔEUC) stratified for implant and scanning device (red= intraoral scanner, blue= stereophotogrammetry)

ments of up to 181.9 μm. Analyzing the 3D deviation into the three space axes, IOS expressed higher deviations on the X-axis (lateral) of 5.21 ± 50.51 μm, while SPG expressed a very high accuracy on the Y-axis (vertical) of 0.95 ±7.15 μm. The extreme IOS deviation values observed in the present study were above the clinically acceptable misfit of 150 μm, which is recommended to prevent long-term mechanical and biological complications[22–24]

Concerning angular deviations, the IOS showed slightly higher mean deviations than the SPG (0.28° vs. 0.24°, $P = 0.0022$), with extreme measurements up to 0.732°.

The reported IOS angular deviations may negatively affect the overall implant-prosthesis fit, particularly in the case of screw-retained complete-arch restorations.

Considering the 3D deviations stratified per implant position, implant 4.5 was the most critical position to be scanned, with IOS deviations up to 181.87 μm, while anterior implants 4.2 and 3.2 were more critical to be scanned for the SPG (deviations up to 80.34 and 77.18 μm).

The intrinsic limitations of the optical surface scanning technology require a consistent and flawless scanning route to reduce the number of images and stitching procedures. Therefore, as advised by the manufacturer of the investigated IOS, the scan should start from the most distal implant and proceed along the dental arch from left to right or right to left.

To facilitate further comparisons, we adopted a previously published scanning strategy[9,19]. The starting point for scanning was the occlusal-lingual surface of the ISB at position 4.5. The scan then moved along the arch toward positions 4.2, 3.2, and 3.5. The scanning process was then reversed, starting from the occlusal-buccal side. Although the IOS starting point usually features better trueness and accuracy, in the present study, position 4.5 was critical because it was characterized as the most challenging position in terms of depth and angulation (depth, -4 mm; distal angulation, 15°), in agreement with previous reports[2].

For all implants except 4.2, the SPG device demonstrated a significant reduction in 3D variability compared to the IOS device. No significant differences were observed between the two devices for implant 4.2. These results confirmed the higher accuracy of SPG, even though a slight reduction in accuracy was noted for the anterior implants for both trueness and precision. This reduction in accuracy for the anterior implant positions led to a similar or higher level of accuracy compared with the IOS. The authors assumed that the worse SPG performance in the anterior implants than in the posterior implants may be related to the scanning mode of the investigated

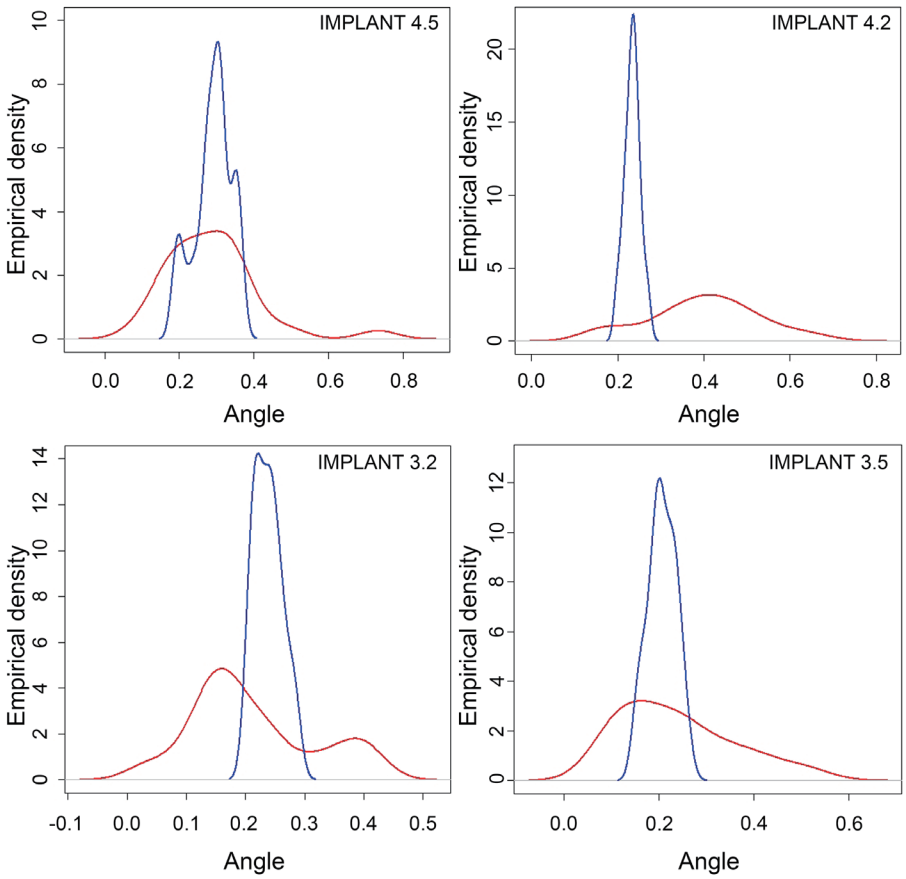

Fig. 6. Empirical distributions of angular discrepancies (ΔANGLE) stratified by implant and scanning device (red= intraoral scanner, blue= stereophotogrammetry)

model. The model being secured on a table prompted the operator to position the SPG device at a 45° angle relative to the dedicated ISB flags. This may explain the worse accuracy recorded for the anterior positions by the SPG compared with the posterior positions. The SPG scanning orientation recommended by the manufacturer should be as close as possible to the dedicated ISB flags screwed onto the implants.

Considering ΔANGLE, no significant difference was found in terms of implant position. The expected angular discrepancy was significantly different between the IOS and SPG only for implant 4.2 (0.40° vs. 0.23°, $P < 0.0001$). However, SPG always performed significantly better than IOS in terms of the SD. Therefore, despite the *in vitro* environment that may have facilitated IOS surface scanning, SPG showed a higher accuracy in both 3D and angular measurements. This is probably because of the different technologies of the two devices. The IOS software elaborates and matches the acquired 3D images through a process known as "stitching," based on a best-fit algorithm. This process was repeated for each image matching and was responsible for the stitching-related deviation for each image coupling. The higher the number of image stitches, the higher the overall error associated with the best-fit alignment[4]. SPG is based on an extraoral device with two infrared charge-coupled device cameras that simultaneously detect a specific optical landmark geometry featuring the surface of each flag ISB, thereby recording the implant coordinates and their spatial relationship in terms of distances and angulations[16]. Because of the larger field of view compared to the currently available IOS devices, SPG simultaneously detects all the implant coordinates and their space relationships with no stitching procedure needed, and is not subject to this type of error source.

Furthermore, SPG, owing to its extraoral scanning approach, is not influenced by any of the intraoral factors reported in the literature, such as the patient's mouth opening, size of the scanner tip, saliva, steam, manufacturing material of the scan bodies, distance between them, and length of the edentulous span and arch. Finally, SPG infrared technology is not affected by ambient light or light reflection[25].

Furthermore, a significantly higher SD was associated with IOS both in terms of 3D deviation (37.1 μm vs. 17.7 μm $P < 0.0001$) and angular deviation (0.14° vs. 0.04° $P < 0.0001$).

According to the SD data for the 3D and angular deviations, the SPG showed much higher precision than the IOS. This evidence demonstrates the dramatically higher recording repeatability of the SPG, which could be explained by the different procedures of the two digital impression devices. The IOS should be adequately moved by the clinician along the arch according to a proper scanning strategy to record all ISB positions and the surrounding gingival anatomy,

thus allowing fast and accurate stitching of the acquired 3D images. SPG is an extraoral digital device that does not need to be moved along the arch but only requires small movements to correctly focus the SPG scan body geometry[26]. Hence, the operator influence is more evident in the use of the IOS and could lead to lower consistency in the measurement procedures. It must be specified that the SPG, as an extraoral scanning device, can detect only the implant positions without recording the surrounding gingival anatomy. For this reason, a second intraoral impression, by means of an IOS or a traditional technique to be digitized later, is necessary to supply the dental technician with a master model that includes all the anatomical information of the edentulous jaw. Moreover, few SPG devices are currently available in the global market, and their cost is higher than that of IOS systems.

To summarize the study findings and their clinical implications:

- The SPG performed better than the IOS in terms of both linear and angular trueness and precision.
- Extreme IOS linear and angular deviations were above the clinically acceptable misfit and may negatively affect the overall implant-prosthesis joint, particularly in screw-retained complete arch restorations.
- The SPG extraoral digital impression is not influenced by any intraoral patient factors, and its infrared technology is not affected by ambient light or light reflection.
- The SPG has a larger field of view than the IOS and simultaneously detects all implant coordinates and their spatial relationship with no stitching procedures.
- Stereophotogrammetry seems to be more feasible for complete arch digital implant impressions than IOS, even though it can only detect implant positions and must be integrated with IOS to record the surrounding gingival anatomy.

5. Conclusions

The SPG complete-arch implant impression showed significantly higher 3D and angular accuracies than the IOS. The SPG showed consistent performance in terms of measurement repeatability. The extreme deviations reported by the IOS were far above the clinically acceptable threshold value, despite the *in vitro* environment that may have facilitated optical surface scanning. Considering the limitations of the current study, stereophotogrammetry appears to be more feasible than IOS for complete arch digital implant impressions. The reported IOS deviations may negatively affect the overall implant-prosthesis fit, particularly in screw-retained complete-arch restorations. Further randomized clinical trials are necessary to investigate the clinical performance of this technology *in vivo*.

Acknowledgments

We wish to thank LaStruttura Spa for the model production and Dr. Andrea Papa for expertise in 3D metrology. We thank the MIUR Excellence Department Project awarded to the Department of Mathematics at the University of Rome, Tor Vergata.

Conflict of interest statement

All the authors declare no potential conflicts of interest in the present scientific paper.

References

[1] Amin S, Weber HP, Finkelman M, El Rafie K, Kudara Y, Papaspyridakos P. Digital vs. conventional full-arch implant impressions: a comparative study. Clin Oral Implants Res. 2017;28:1360–7. https://doi.org/10.1111/clr.12994, PMID:28039903

[2] Rutkūnas V, Gečiauskaitė A, Jegelevičius D, Vaitiekūnas M. Accuracy of digital implant impressions with intraoral scanners. A systematic review. Eur J Oral Implantology. 2017;10(suppl 1):101–20. PMID:28944372

[3] Logozzo S, Zanetti EM, Franceschini G, Kilpelä A, Mäkynen A. Recent advances in dental optics – Part I: 3D intraoral scanners for restorative dentistry. Opt Lasers Eng. 2014;54:203–21. https://doi.org/10.1016/j.optlaseng.2013.07.017

[4] Kihara H, Hatakeyama W, Komine F, Takafuji K, Takahashi T, Yokota J, *et al*. Accuracy and practicality of intraoral scanner in dentistry: A literature review. J Prosthodont Res. 2020;64:109–13. https://doi.org/10.1016/j.jpor.2019.07.010, PMID:31474576

[5] Imburgia M, Logozzo S, Hauschild U, Veronesi G, Mangano C, Mangano FG. Accuracy of four intraoral scanners in oral implantology: a comparative in vitro study. BMC Oral Health. 2017;17:92. https://doi.org/10.1186/s12903-017-0383-4, PMID:28577366

[6] Revilla-León M, Kois DE, Kois JC. A guide for maximizing the accuracy of intraoral digital scans. Part 1: operator factors. J Esthet Restor Dent. 2023;35:230–40. https://doi.org/10.1111/jerd.12985, PMID:36479807

[7] Revilla-León M, Kois DE, Kois JC. A guide for maximizing the accuracy of intraoral digital scans: Part 2—Patient factors. J Esthet Restor Dent. 2023;35:241–9. https://doi.org/10.1111/jerd.12993, PMID:36639916

[8] Flügge T, Att W, Metzger M, Nelson K. Precision of dental implant digitization using intraoral scanners. Int J Prosthodont. 2016;29:277–83. https://doi.org/10.11607/ijp.4417, PMID:27148990

[9] Arcuri L, Pozzi A, Lio F, Rompen E, Zechner W, Nardi A. Influence of implant scanbody material, position and operator on the accuracy of digital impression for complete-arch: A randomized in vitro trial. J Prosthodont Res. 2020;64:128–36. https://doi.org/10.1016/j.jpor.2019.06.001, PMID:31255546

[10] Revilla-León M, Att W, Özcan M, Rubenstein J. Comparison of conventional, photogrammetry, and intraoral scanning accuracy of complete-arch implant impression procedures evaluated with a coordinate measuring machine. J Prosthet Dent. 2021;125:470–8. https://doi.org/10.1016/j.prosdent.2020.03.005, PMID:32386912

[11] Pozzi A, Arcuri L, Lio F, Papa A, Nardi A, Londono J. Accuracy of complete-arch digital implant impression with or without scanbody splinting: an in vitro study. J Dent. 2022;119:104072. https://doi.org/10.1016/j.jdent.2022.104072, PMID:35189313

[12] Lie A, Jemt T. Photogrammetric measurements of implant positions. Description of a technique to determine the fit between implants and superstructures. Clin Oral Implants Res. 1994;5:30–6. https://doi.org/10.1034/j.1600-0501.1994.050104.x, PMID:8038342

[13] Jemt T, Lie A. Accuracy of implant-supported prostheses in the edentulous jaw. Analysis of precision of fit between cast gold-alloy frameworks and master casts by means of a three-dimensional photogrammetric technique. Clin Oral Implants Res. 1995;6:172–80. https://doi.org/10.1034/j.1600-0501.1995.060306.x, PMID:7578793

[14] Jemt T, Bäck T, Petersson A. Photogrammetry--an alternative to conventional impressions in implant dentistry? A clinical pilot study. Int J Prosthodont. 1999;12:363–8. PMID:10635208

[15] Agustín-Panadero R, Peñarrocha-Oltra D, Gomar-Vercher S, Peñarrocha-Diago M. Stereophotogrammetry for recording the position of multiple implants: Technical description. Int J Prosthodont. 2015;28:631–6. https://doi.org/10.11607/ijp.4146, PMID:26523726

[16] Gómez-Polo M, Gómez-Polo C, del Río J, Ortega R. Stereophotogrammetric impression making for polyoxymethylene, milled immediate partial fixed dental prostheses. J Prosthet Dent. 2018;119:506–10. https://doi.org/10.1016/j.prosdent.2017.04.029, PMID:28709673

[17] Tohme H, Lawand G, Chmielewska M, Makhzoume J. Comparison between stereophotogrammetric, digital, and conventional impression techniques in implant-supported fixed complete arch prostheses: An in vitro study. J Prosthet Dent 2021;S0022-3913(21)00269-9.

[18] Ma B, Yue X, Sun Y, Peng L, Geng W. Accuracy of photogrammetry, intraoral scanning, and conventional impression techniques for complete-arch implant rehabilitation: an in vitro comparative study. BMC Oral Health. 2021;21:636. https://doi.org/10.1186/s12903-021-02005-0, PMID:34893053

[19] Müller P, Ender A, Joda T, Katsoulis J. Impact of digital intraoral scan strategies on the impression accuracy using the TRIOS Pod scanner. Quintessence Int. 2016;47:343–9. https://doi.org/10.3290/j.qi.a35524, PMID:26824085

[20] Mizumoto RM, Yilmaz B, McGlumphy EA Jr, Seidt J, Johnston WM. Accuracy of different digital scanning techniques and scan bodies for complete-arch implant-supported prostheses. J Prosthet Dent. 2020;123:96–104. https://doi.org/10.1016/j.prosdent.2019.01.003, PMID:31040026

[21] Rutkunas V, Gedrimiene A, Akulauskas M, Fehmer V, Sailer I, Jegelevicius D. In vitro and in vivo accuracy of full-arch digital implant impressions. Clin Oral Implants Res. 2021;32:1444–54. https://doi.org/10.1111/clr.13844, PMID:34543478

[22] Schwarz MS. Mechanical complications of dental implants. Clin Oral Implants Res. 2000;11(suppl 1):156–8. https://doi.org/10.1034/j.1600-0501.2000.011S1156.x, PMID:11168264

[23] Aglietta M, Siciliano VI, Zwahlen M, Brägger U, Pjetursson BE, Lang NP, *et al.* A systematic review of the survival and complication rates of implant supported fixed dental prostheses with cantilever extensions after an observation period of at least 5 years. Clin Oral Implants Res. 2009;20:441–51. https://doi.org/10.1111/j.1600-0501.2009.01706.x, PMID:19522975

[24] Pozzi A, Arcuri L, Fabbri G, Singer G, Londono J. Long-term survival and success of zirconia screw-retained implant-supported prostheses for up to 12 years: A retrospective multicenter study. J Prosthet Dent. 2023;129:96–108. https://doi.org/10.1016/j.prosdent.2021.04.026

[25] Peñarrocha-Diago M, Balaguer-Martí JC, Peñarrocha-Oltra D, Balaguer-Martínez JF, Peñarrocha-Diago M, Agustín-Panadero R. A combined digital and stereophotogrammetric technique for rehabilitation with immediate loading of complete-arch, implant-supported prostheses: A randomized controlled pilot clinical trial. J Prosthet Dent. 2017;118:596–603. https://doi.org/10.1016/j.prosdent.2016.12.015, PMID:28385445

[26] Pradíes G, Ferreiroa A, Özcan M, Giménez B, Martínez-Rus F. Using stereophotogrammetric technology for obtaining intraoral digital impressions of implants. J Am Dent Assoc. 2014;145:338–44. https://doi.org/10.14219/jada.2013.45, PMID:24686966

Received: 11 February 2023 | Revised: 4 July 2023 | Accepted: 13 July 2023

DOI: 10.1111/clr.14141

ORIGINAL ARTICLE

CLINICAL ORAL IMPLANTS RESEARCH WILEY

Accuracy of complete-arch digital implant impression with intraoral optical scanning and stereophotogrammetry: An in vivo prospective comparative study

Alessandro Pozzi[1,2] | Paolo Carosi[3] | German O. Gallucci[4] | Katalin Nagy[5] | Alessandra Nardi[6] | Lorenzo Arcuri[7]

[1]Department of Clinical Sciences and Translational Medicine, School of Dentistry, University of Tor Vergata, Rome, Italy

[2]Departement of Restorative Sciences, Dental College of Georgia, Augusta University, Augusta, USA

[3]Department of Chemical Science and Technologies, PhD in Materials for Health, Environment and Energy – Dentistry, University of Rome Tor Vergata, Rome, Italy

[4]Department of Restorative Dentistry and Biomaterials Sciences, Harvard School of Dental Medicine, Boston, Massachusetts, USA

[5]Department of Oral Surgery, Faculty of Dentistry, University of Szeged Tisza L. Krt, Szeged, Hungary

[6]Department of Mathematics, University of Rome Tor Vergata, Rome, Italy

[7]Department of Odontostomatological and Maxillofacial Sciences, Sapienza University of Rome, Rome, Italy

Correspondence
Alessandro Pozzi, Department of Restoratice Sciences. Dental College Georgia, Augusta University, USA.
Email: apozzi@augusta.edu

Abstract

Objectives: To assess accuracy of intraoral optical scanning (IOS) and stereophotogrammetry (SPG), complete-arch digital implant impressions in vivo.

Materials and Methods: Consecutive patients needing implant-supported screw-retained zirconia complete-arch fixed-dental prostheses (ISZ-FDP) were recruited. For each patient, three impressions were taken: IOS, SPG (tests), and open-tray plaster (reference). Linear (ΔX, ΔY, and ΔZ), three-dimensional (ΔEUC), and angular deviations (ΔANGLE) were evaluated and stratified according to scanning technology for each implant. Potential effects of impression device (IOS and SPG), arch (maxilla and mandible), and implant number (4 and 6) were evaluated through multivariable analysis. Significance level was set at .05.

Results: A total of 11 complete arches (5 maxillae, 6 mandibles) in 11 patients were rehabilitated with ISZ-FDPs supported by 4 ($n=8$) and 6 implants ($n=3$). A total of 50 implants and 100 implant positions were captured by two investigated devices and compared to respective reference (mean ΔEUC IOS 137.2, SPG 87.6 µm; mean ΔANGLE 0.79, 0.38°). Differences between measurements (SPG-IOS) were computed for each implant, with negative values indicating better SPG accuracy. Significant mean ΔEUC difference of −49.60 µm ($p=.0143$; SD 138.15) and mean ΔANGLE difference of −0.40° ($p<.0001$; SD 0.65) were observed in favor of SPG. Multivariable analysis showed significant effect on ΔEUC ($p=.0162$) and ΔANGLE ($p=.0001$) only for impression devices, with SPG performing better.

Conclusions: SPG experienced significantly higher linear and angular accuracy. No effect of type of arch or implant number was detected. Higher extreme deviations were experienced for IOS. SPG can be feasible for complete-arch digital impressions with caution, and rigid prototype try-in is recommended before screw-retained prosthesis manufacturing.

KEYWORDS
complete arch, dental implant, digital impression, intraoral scanner, stereophotogrammetry

1 | INTRODUCTION

Screw-retained complete-arch fixed-dental prostheses (FDPs) need accurate matching between implants and frameworks to achieve long-term successful outcomes (Sanda et al., 2021). The target is to deliver an FDP that properly fits the prosthetic platforms without static loads to minimize the occurrence of mechanical complications (Arcuri et al., 2020; Rungruanganunt et al., 2013). A passive fit with an accuracy of up to 150 μm is strongly advised (Jemt & Lie, 1995; Pozzi et al., 2022; Pradíes et al., 2014). However, a prosthetic misfit may lead to bacterial leakage and cause biological complications (Katsoulis et al., 2017); therefore, an accurate recording of the implant coordinates and prosthetic manufacturing are fundamental prerequisites (Aglietta et al., 2009; Pradíes et al., 2014).

The conventional implant impression workflow is still considered the gold standard for complete arches (Pozzi, Tallarico, Mangani, et al., 2013). However, several steps are necessary to produce the master cast, and each step is accountable for errors due to the intrinsic limitations of impression and pouring materials (Pozzi, Tallarico, Mangani, et al., 2013). The further need to digitize the master cast for computer-aided design–computer-aided manufacturing (CAD-CAM) makes the overall workflow even more challenging (Yan et al., 2022). To avoid these issues and shorten the overall digital workflow, an intraoral optical surface scanning (IOS) implant impression was introduced to record and directly digitize the implant positions (Peñarrocha-Diago et al., 2017).

Digital impressions are now considered a valid alternative to conventional impressions to record intraoral anatomy and implant positions (Amin et al., 2017; Rutkūnas et al., 2017). However, IOS implant impression accuracy has been proven reliable for single and short spam FDPs (Imburgia et al., 2017). Accuracy is defined by trueness and precision (ISO5725-1); trueness describes the conformity of measurements to the actual values, and precision describes the conformity of multiple repeated measurements (Flügge et al., 2016). The application of IOS for complete-arch implant impression is still considered controversial both in terms of accuracy and practicality, especially for the lower jaw (Arcuri et al., 2020; Revilla-León et al., 2021). The major limitation of the current IOS systems is intrinsic to the three-dimensional (3D) image reconstruction technology, which is based on the best-fit algorithm stitching process. Continuous reference points are necessary to speed up the stitching process and increase the matching accuracy of the acquired consecutive 3D images (Kihara et al., 2019; Pozzi et al., 2022). Consequently, different artificial landmark techniques have been proposed and tested positively in terms of accuracy but are not free of deviations and may be cumbersome (Huang et al., 2020; Pozzi et al., 2022).

Stereophotogrammetry (SPG) was reported as a different digital impression technology to simultaneously record 3D objects and their spatial relationship using points within photographic images captured by two stereo cameras (Gómez-Polo et al., 2018). SPG was first proposed by Lie and Jemt (1994) as a method to measure the misfit between implants and frameworks. The use of SPG was proven to be a reliable guided surgery technology to execute a digitally planned implant treatment by a stereo tracking algorithm linking the preoperative implant planning coordinates with the live-tracked drilling and positioning coordinates system (Pozzi, Arcuri, Carosi, et al., 2021). SPG digital impression can record only the implant coordinates, and no stitching process is needed; however, recording of the intraoral dental and gingival anatomy is not possible and must be integrated with an auxiliary impression (Agustín-Panadero et al., 2015).

In vitro studies analyzed SPG accuracy for complete-arch implant impressions reporting controversial results (Ma et al., 2021; Revilla-León et al., 2021).

To the best of our knowledge, this is the first in vivo prospective clinical trial whose primary aim was to investigate and compare the accuracy of IOS and SPG for complete-arch implant impression. The clinical performance of IOS and SPG was evaluated for each patient enrolled in the study with a paired comparison of the deviation differences. The secondary aim was to analyze the potential effect of the type of arch (maxilla vs. mandible) and number of implants (4 vs. 6) on SPG and IOS accuracy. The null hypothesis was that SPG and IOS would show equivalent accuracy.

2 | MATERIALS AND METHODS

Since November 2020, any patient, of both genders, aged 18 years or older and in need of complete-arch FDPs, was recruited and enrolled in the clinical study. Informed consent was obtained from each enrolled patient. The nature of the study, benefits, risks, and possible alternative treatments were widely commented on prior to inclusion in the study, as well as any follow-up evaluations needed. Patients were consecutively treated up to April 2021 in one rehabilitation center.

The clinical trial was approved by the ethical committee of the University of Rome Tor Vergata (Protocol number 203.20) and registered as clinical trial in ISRCTN (https://www.isrctn.com) with number ISRCTN12501259, conducted in compliance with the Declaration of Helsinki for biomedical research involving human subjects as amended in 2008 and according to the industry regulations (the International Conference for Harmonization Guideline for Good Clinical Practice and ISO14155). According to the university institution regulations, study data are in the university repository and are not publicly available to avoid compromising ethical standards and legal requirements. Peer review of empirical data was conducted by an independent examiner member of the scientific committee of the University of Rome Tor Vergata to confirm the quality of the shared data and to confirm that the data reproduce the analytic results reported in the paper: (1) sample sizes match, (2) the variables described in the article are present as fields in the data university repository, (3) data are complete; (4) data are properly labelled and described; (5) it has the appropriate metadata for the kind of data being shared; and (6) data are available on request from the corresponding author.

The following inclusion criteria were used: (1) medically healthy patients; (2) full-mouth bleeding and full-mouth plaque index lower than or equal to 25%; (3) bone height for at least 10-mm-long implants; (4) bone width of at least 5 and 6 mm for narrow (NP 3.75 mm) and regular (RP 4.3 mm) implants, respectively; (5) fresh extraction sockets with an intact buccal wall; (6) at least 4 and 5 mm of bone beyond the root apex in the mandible and maxilla; (7) minimal insertion torque of 45 Ncm; (8) minimal Implant Stability Quotient (ISQ) mean value of 64 on the day of the surgery; (9) same-day surgery and provisionalization; (10) screw-retained complete-arch FDPs supported by 4 and 6 implants in the maxilla and/or mandible; (11) ISQ mean value of 72 the day of the definitive impression; and (12) availability to attend regular follow-up visits. Exclusion criteria were general medical (American Society of Anesthesiologists, ASA, class III or IV) and/or psychiatric contraindications; pregnancy or nursing; any interfering medication such as steroid therapy or bisphosphonate therapy; alcohol or drug abuse; heavy smoking (>10 cigarettes/day), radiation therapy to head or neck region within 5 years, and untreated periodontitis; acute and chronic infections of the adjacent tissues or natural dentition; severe maxillomandibular skeletal discrepancy; high and moderate parafunctional activity; and absence of opposite teeth (Johansson et al., 2011).

One clinician for each center performed all the surgical and prosthetic procedures, and one dental laboratory experienced in CAD-CAM technology designed and manufactured the screw-retained zirconia ceramic implant-supported prostheses. This study is reported in accordance with the Strengthening the Reporting of Observational Studies in Epidemiology (STROBE) statement for improving the quality of observational studies (http://www.strobe-statement.org; von Elm et al., 2014) (Supporting Information).

2.1 | Clinical and laboratory protocol

Before implant placement, all study participants received a comprehensive examination including a cone-beam computed tomography scan. The digital imaging and communication in medicine (DICOM) files were imported into the implant planning software program (DTXStudioImplant; Dexis). Implant planning was executed accurately according to a prosthetically and soft tissue-driven approach, positioning the two anterior implants parallel to each other and the two or four posterior implants angulated symmetrically with the same divergence with respect to the anteriors (Agliardi et al., 2012, 2023; Pozzi, Arcuri, et al., 2020). Conical connection implants (NobelActive, NobelParallel; NobelBiocare AG) were placed by means of computer-assisted static and dynamic-guided surgery (Pozzi, Hansson, et al., 2020). A digitally prefabricated multilayered polymethyl methacrylate (Whitepeaks; Whitepeaks Dental Solutions GmbH & Co) interim prosthesis was relined on temporary cylinders screwed at the abutment level (MUA abutment; NobelBiocare AG) and delivered on the day of the surgery. After an uneventful healing period of 3 and 4 months in the mandible and the maxilla, the provisional restoration was removed, and the implant stability quotient was measured. In the case of ISQ > 72, abutment-level impression copings were tightened onto the multiunit abutments at 15 Ncm, and a conventional definitive impression was made with an open-tray technique and plaster material (SnowWhite Plaster no. 2; Kerr) (Pozzi, Tallarico, Mangani, et al., 2013) (Figures 1 and 2). The master casts were poured from the conventional plaster impression in low expansion type IV dental stone (FujiRock EP; GC). The master cast were digitalized with a high-resolution laboratory scanner (D2000; 3Shape), with an accuracy of 5 µm, as specified by the International Organization for Standardization (ISO) standard 12836 to achieve digital master cast standard tessellation language (STL) file used as reference. International Organization for Standardization, ISO 9693-1 (Dentistry compatibility testing. Part 1: Metal–ceramic systems. Geneva: International Organization for Standardization; 2012. ISO Store Order: OP-184149 (Date: 2017-06-09). Available at: http://www.iso.org/iso/home.html). Then, an IOS impression was recorded with an intra-oral scanner (TRIOS4; 3Shape A/S) using implant scan bodies secured at the multiunit abutment level (Elos Accurate Multi-Unit; Elos Medtech) (Figure 3). The IOS device was a wireless pen-grip, powder-free scanner based on confocal microscopy laser technology with software version 1.4.7.5 calibrated right before the impression. The scan strategy was consistent for all the procedures following the manufacturer guidelines and starting from the most distal implant scan body on the patient's left side. The SPG system (Precise Implant capture, PiC camera, PiC dental) consisted of two charged couple device cameras designed and optimized for clinical use to identify specific scan bodies with single encoding secured onto the multiunit abutments (Figure 4). The SPG device has an infrared flash to eliminate shadow cast by ambient light, and the two cameras captured 10 extra-oral photographs per second with an error margin lower than 10 µm. Before the scan, each SPG scan body was identified according to its surface code, selected into the software, and screwed onto the multiunit abutments (Figure 5). The SPG system was positioned extra-orally, 15–30 cm from the patient's mouth, and with an angulation variable from 90° to 45° with respect

FIGURE 1 Scalloped soft-tissue profile of treated maxilla at definitive multiunit-level impression.

FIGURE 2 Plaster open-tray definitive impression.

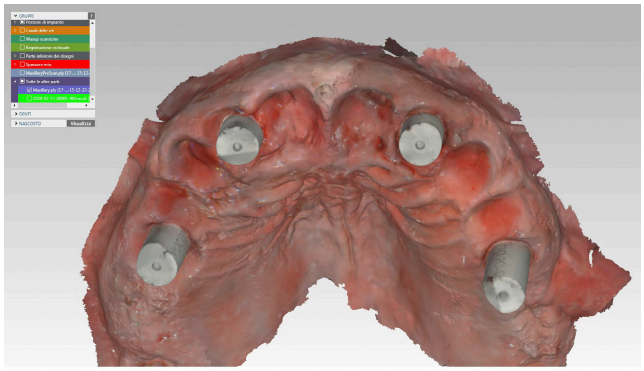

FIGURE 3 Intraoral optical scanning digital impression using implant scan bodies secured at the multiunit abutment level.

FIGURE 4 Clinical scenario of stereophotogrammetry system recording digital coordinates of specific scan bodies secured onto the multiunit abutments.

to the scan body surface to have all the SPG scan body geometries in the sight of the two stereo cameras (Figure 4). After internal system calibration, the images captured by the SPG system were processed, and the software algorithm extracted the relative angle and distance between each implant position in vector form. The SPG impression recorded only the vectorial relationship between the implant prosthetic platforms in an STL file (Figure 6) and had to be integrated with the soft-tissue information achieved by the IOS impression using a best-fit software algorithm (DTX StudioLab; Dexis).

FIGURE 5 Intraoral view of the stereophotogrammetry scan bodies. Note that each scan body has a unique code that is provided by the position of the white dots on its surface.

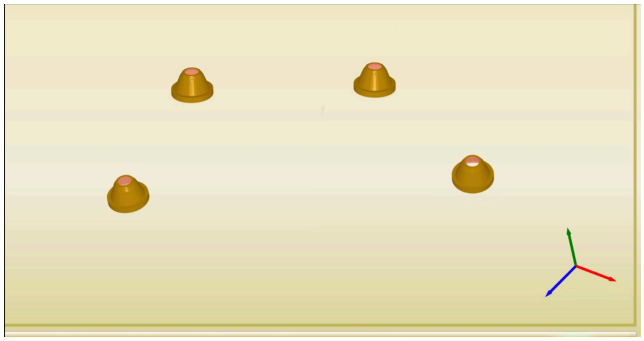

FIGURE 6 Implant prosthetic platforms standard tessellation language digital coordinates elaborated by stereophotogrammetry software after the digital impression.

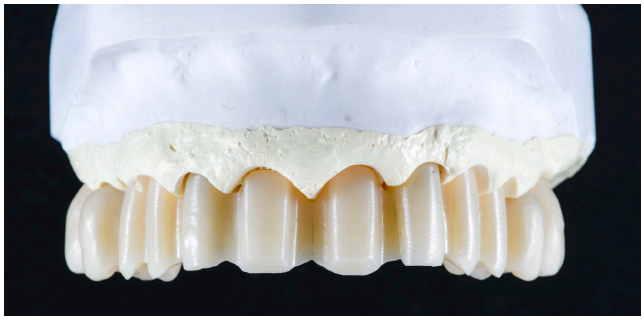

FIGURE 7 Implant-supported screw-retained zirconia-based complete-arch fixed-dental prostheses made by computer-aided design/computer-aided manufacturing procedures at the moment of accuracy and fit of assessment onto plaster master cast.

CAD-CAM implant-supported screw-retained zirconia-based complete-arch FDPs (ISZ-FDPs) were digitally designed onto master cast reference files, obtained from the plaster impression, and fabricated by centralized industrial production (NobelBiocare Procera LL) (Figure 7). The accuracy and fit of ISZ-FDP were first assessed onto the respective master cast using a dental laboratory microscope (Leica M50; Leica Microsistems) at 35× magnification and the

Sheffield one-screw test and then in the patient mouth according to established criteria, such as strain-free screwing, as well as no open margins at the clinical and radiographic examinations during the Sheffield one-screw test performed chair side (framework correctly in place without vertical and horizontal discrepancy at close-up inspection and periapical radiographs) (Figures 8a,b and 9) (Abduo et al., 2010; Kan et al., 1999; Pozzi, Arcuri, Fabbri, et al., 2021; Pozzi, Tallarico, & Barlattani, 2013).

2.2 | Data processing and accuracy assessment

All the ISZ-FDPs passed the accuracy and fit test. For each patient complete arch, three digital files were obtained: one reference scan (indirect digitalization of plaster impression) and two test scans (IOS and SPG digital impressions). The digital files including only the implant positions were then used for the accuracy analysis. The IOS and SPG test scans of each patient's complete arch were aligned to the relative reference scan with a Gauss best-fit algorithm (Geomagic Studio 12; 3DSystems), with an alignment tolerance of 0.01 mm, and two alignment optimizations were accomplished after file superimposition (Peroz et al., 2021). Linear (ΔX, ΔY, and ΔZ) and angular deviations (ΔANGLE) between the test scan and reference scan were measured for any implant position, analyzing the previously superimposed files by means of dedicated software (Hyper Cad S, Cam HyperMill, Open Mind Technologies). Negative values on the *X*, *Y*, and *Z* axes described an implant positioned left, downwards, and backwards, respectively (lateral, vertical, and longitudinal), while the positive values were in the opposite direction on each axis. Three-dimensional (3D) deviation was calculated for each implant position according to the Euclidean distance (ΔEUC).

2.3 | Statistical analysis

Assuming Euclidean distance as the primary endpoint and a significance level of .05, $n = 84$ was the minimum sample size able to guarantee, for a minimum expected difference of 120 μm (SD 150 μm), and a test power of 0.95. Sample size computation was based on paired *t*-test. The mean, SD, and minimum and maximum values were reported to summarize continuous variables. Differences between errors associated with the two devices (SPG-IOS) were computed for each implant with negative values expressing a benefit in terms of accuracy in favor of SPG. Their empirical distributions were obtained by Kernel density estimator; significance was evaluated by paired *t*-test. ANOVA was used to compare expected differences among the three groups. Box and Whisker plots were created to graphically compare empirical distributions. Multivariable analysis was based on the mixed linear model. Two different models were fitted assuming ΔEUC and ΔANGLE as response variables; logarithmic transformation was applied to improve normality. In both models, the fixed effects of scanning device (IOS vs. SPG), type of arch (maxilla vs. mandible), and supporting implant number (4 implants vs. 6 implants) were assessed. All analyses were undertaken using SAS software version 9.4 (SAS Institute) and R version 3.4.

3 | RESULTS

Eleven edentulous arches (five maxillae, six mandibles) in 11 patients were rehabilitated with screw-retained implant prostheses supported by 4 ($n = 8$) and 6 implants ($n = 3$) for a total amount of 50 implants. Implant positions were scanned by means of two digital devices (IOS and SPG) for a total of 100 implant positions recorded to be compared to the relative reference scans. Deviations were evaluated over the *Y*-, *X*-, and *Z*-axes, and angulation and stratified according to the scanning device (Table 1). Table 1 describes in detail the deviations from the reference scans of the IOS and SPG. The mean errors associated with the use of SPG are always less than those related to IOS except for ΔX. Note also the difference in terms of SD both on the linear and angular deviation in favor of SPG. For each implant, the difference between the ΔEUC associated with the two devices (SPG–IOS) was computed; the empirical distribution is shown in Figure 10. A mean difference of −49.60 μm (SD 138.15) was observed with a significant error reduction for SPG compared to IOS ($p = .0143$). The difference distribution was stratified by the type of arch and implant number (Figure 11). Note that no mandible with 6 implants is present in the sample. Although no significant difference was detected among

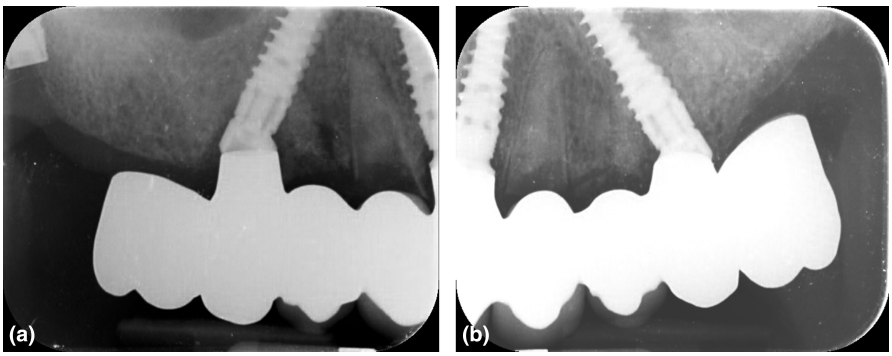

FIGURE 8 (a, b) Periapical radiographs to assess the correct fit of the ISZ-FDP in the patient's mouth during the Sheffield one-screw test. ISZ-FDP, implant-supported screw-retained zirconia-based complete-arch fixed-dental prostheses.

FIGURE 9 Clinical view after definitive restoration placement.

TABLE 1 Descriptive analysis of IOS and SPG linear, 3D, and angular deviations.

	Mean	SD	Min	Max
IOS				
Δ*X* (μm)	−19.8	110.2	−223	304.7
Δ*Y* (μm)	−4.1	44.3	−111.6	−147.1
Δ*Z* (μm)	−41.9	127.5	−536.3	177.6
ΔEUC (μm)	137.2	115.5	11.5	558.1
Angle (°)	0.79	0.59	0.05	2.89
SPG				
Δ*X* (μm)	−24.8	71.8	−192	113.8
Δ*Y* (μm)	−3.4	29	−173.8	50.8
Δ*Z* (μm)	20.9	79.1	−264	250.8
ΔEUC (μm)	87.6	74.2	12	316.2
Angle (°)	0.38	0.29	0.02	1.92

Abbreviations: IOS, intraoral optical scanning; SPG, stereophotogrammetry.

the three groups ($p = .5925$), three extreme differences were observed for mandible and 4 implants with impressive differences in favor of SPG (Table 2).

Considering the difference distribution for ΔANGLE (Figure 12), a mean deviation difference of −0.40° (SD 0.65°) was observed with a significant positive effect of SPG ($p < .0001$).

In the stratified analysis, no significant difference among groups was detected ($p = .2666$) (Figure 13).

Note that three extreme differences in angular accuracy were observed in favor of SPG of approximately −2.75, −1.90, and −1.62° (Table 3). In the multivariable analysis, two different mixed linear models were fitted, considering ΔEUC and ΔANGLE as response variables. In both models, the scanning device (IOS vs. SPG), type of arch (maxilla vs. mandible), and implant number (4 implants vs. 6 implants) were assumed as explanatory variables. The scanning device confirmed a significant effect on both ΔEUC and ΔANGLE; the *p*-values were .0162 and .0001, respectively (Tables 4 and 5). No significant effect was detected for the type of arch and supporting implant number. Note that in the case of ΔANGLE, parameter estimates for type of arch and implant number are close to 0, while for ΔEUC, both estimated effects and standard errors are consistent.

4 | DISCUSSION

The use of complete-arch digital implant impression is still controversial due to the current paucity of data, with only two in vivo studies comparing SPG and IOS technologies (Orejas-Perez et al., 2022; Yan et al., 2022). The primary objective of this single cohort clinical trial was to investigate and compare the accuracy of IOS and SPG for complete-arch digital implant impression. The secondary objective was to analyze the potential effect of the type of arch (maxilla vs. mandible) and number of implants (4 vs. 6) on SPG and IOS accuracy. The main limitation is that reported outcomes are inherent to the investigated IOS and SPG systems and shall be extrapolated with caution to any other device. However, the authors investigated one of the two SPG devices commercially available and one of the most widely published IOS in the scientific literature. Furthermore, one expert clinician performed all the scans, which may have unidentified some differences between the systems related to operator skill and experience. To the best of our knowledge, this is the first clinical trial assessing accuracy of complete-arch digital impressions executed with two investigated devices with sample size calculation and powerful statistics. An a priori sample size was difficult to define being the first study in vivo. Assuming Euclidean distance as the primary endpoint and a significance level of .05, it was computed a sample size of $n = 84$ as the minimum sample size able to guarantee, a minimum expected difference of 120 μm (SD 150 μm), and a test power of 0.95. During the study execution, it was able to increase the total sample to $n = 100$ (50 implant positions per device), corresponding to 11 complete arches (5 maxillae, 6 mandibles) in 11 patients analyzed in accordance with principles of good clinical practice and documented with no protocol deviations. Despite the relative low patient sample size, a total of three impressions (plaster, SPG, and IOS) was taken in each patient enrolled in the study, and the clinical performance of IOS and SPG was evaluated with a paired comparison of the deviation differences for each implant position. Even though sample size was limited, a non-significant test does not prove the absence of an effect, especially if of small magnitude. However, at multivariable analysis, it was able to identify a significant effect for the scanning device, after adjusting for type of arch and implant number. Similarly, an important effect of type of arch and implant number would have been detected if large in magnitude. Nevertheless, the sample was increased, the ratio between the number of patients and investigated variables (device, type of arch, and implant number) has to be considered as a limiting factor, and future research with a greater patient sample size is advised to further confirm the results achieved in the present study. The use of a certified 5 μm accuracy optical desk scanner as a reference, with its limitations, was justified by the better access to the freedom planes compared to tactile systems such as the coordinate measuring machine and because it is widely accepted as a laboratory procedure to digitize the plaster master cast (Mizumoto et al., 2020). The study design was based on the use of a Gauss best-fit alignment

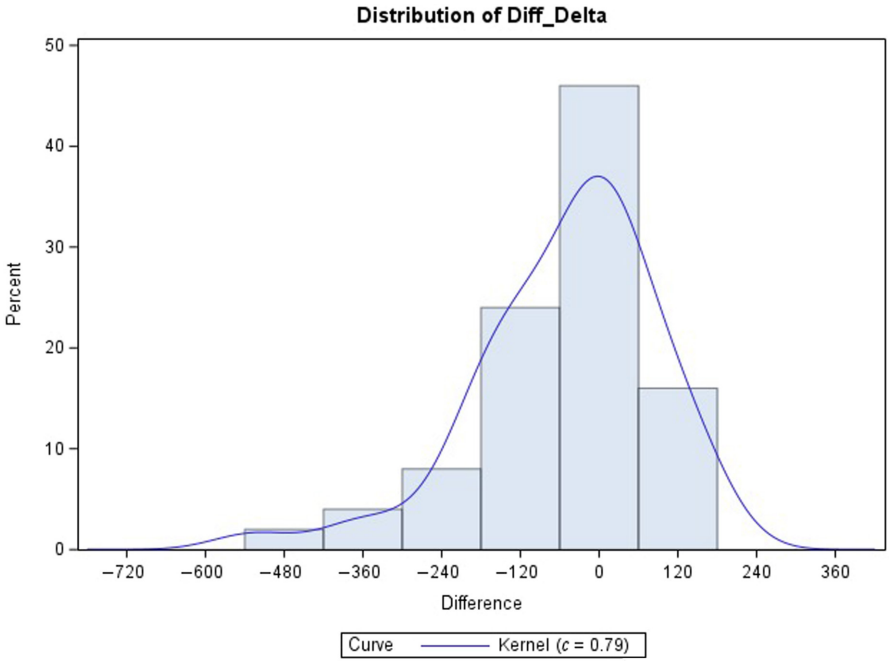

FIGURE 10 Empirical distribution of ΔEUC difference between stereophotogrammetry and intraoral optical scanning.

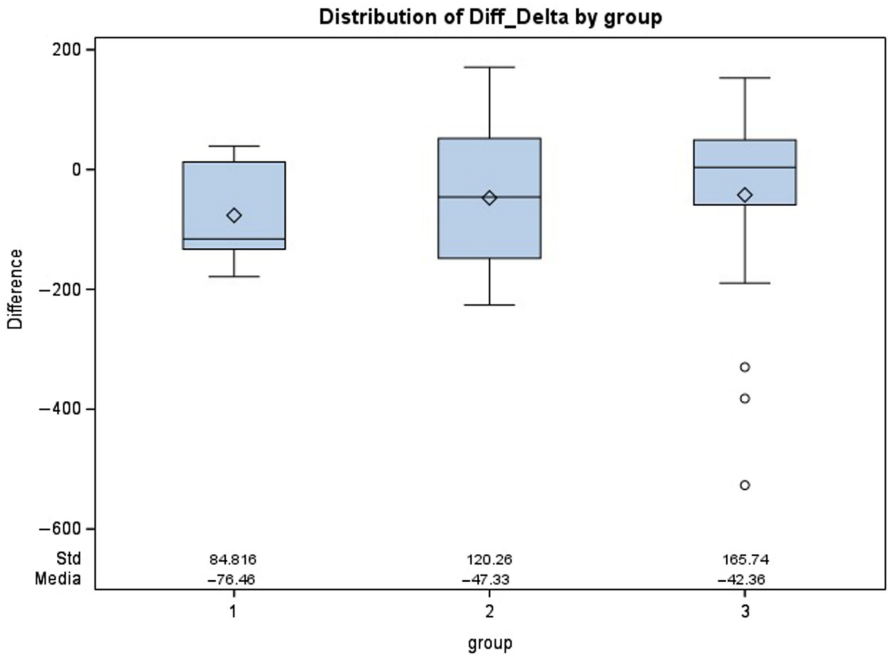

FIGURE 11 Distribution of ΔEUC difference between stereophotogrammetry and intraoral optical scanning according to type of arch and implant number: 1 = maxilla with 4 implants, 2 = maxilla with 6 implants, and 3 = mandible with 4 implants.

TABLE 2 ΔEUC extreme differences cases (μm).

Obs	SPG	IOS	ΔEUC difference	Patient	Arch	Support	Implant
24	31.2107	558.082	−526.871	5	Mandible	4 Implants	24
31	30.1874	359.980	−329.793	7	Mandible	4 Implants	31
39	25.7195	407.929	−382.209	9	Mandible	4 Implants	39

Abbreviations: IOS, intraoral optical scanning; SPG, stereophotogrammetry.

algorithm between the reference and test scans to measure the deviations for each implant position and to further analyze the 3D deviation in each of the three space axes. The Gauss best-fit algorithm, termed also iterative closest point alignment, allowed deviation measurement of all implant positions comparing the respected test and reference files and was proven to be a superior measurement method compared to other alignment algorithms (Peroz et al., 2021). In that way, it was possible to properly analyze the deviations of each implant from a linear (Δ*Y*, Δ*X*, Δ*Z*), 3D (ΔEUC), and angular point of view (ΔANGLE).

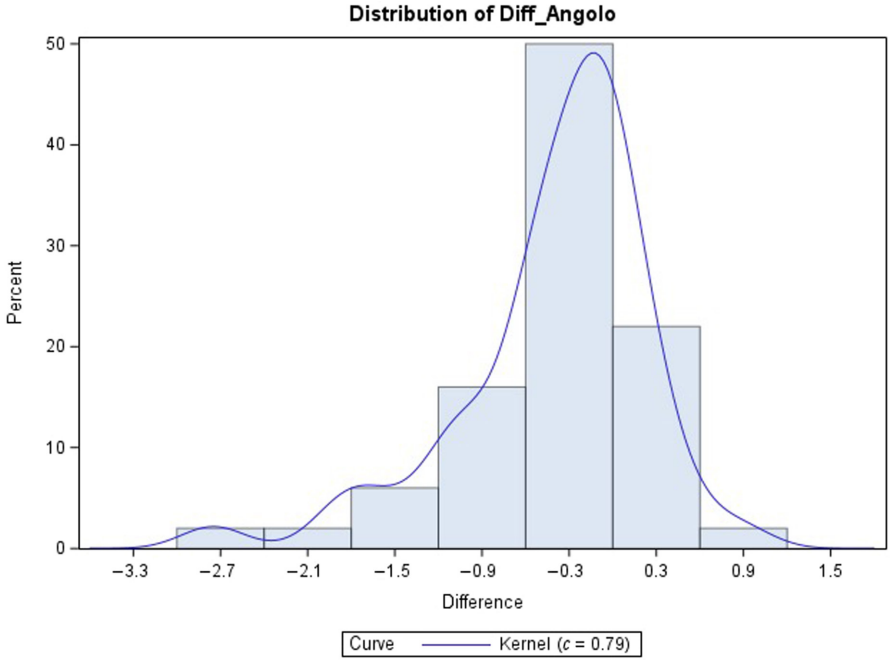

FIGURE 12 Empirical distribution of ΔANGLE difference between stereophotogrammetry and intraoral optical scanning.

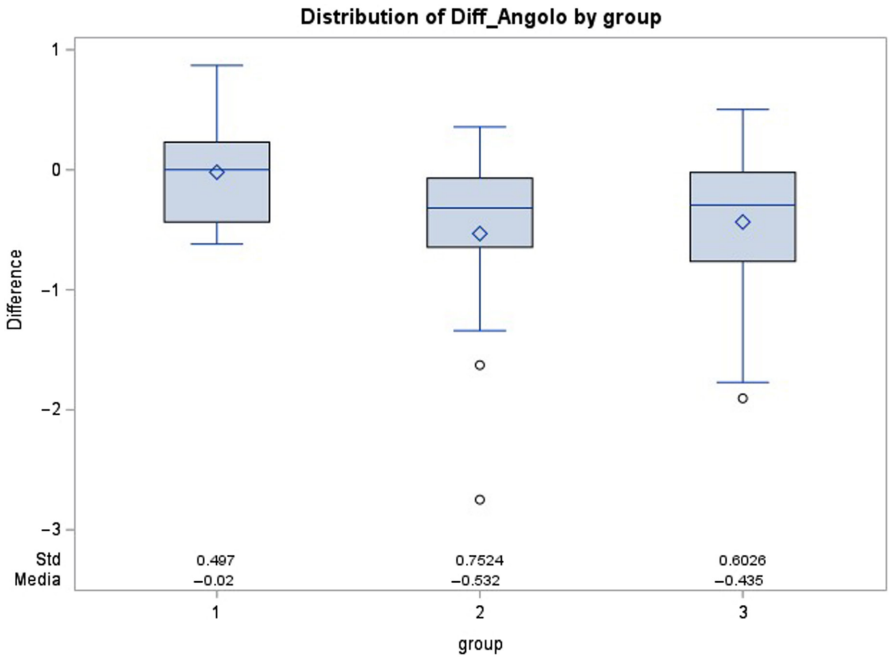

FIGURE 13 Distribution of ΔANGLE difference between stereophotogrammetry and intraoral optical scanning according to type of arch and implant number: 1 = maxilla and 4 implants, 2 = maxilla and 6 implants, and 3 = mandible and 4 implants.

TABLE 3 ΔANGLE extreme differences cases (°).

Obs	SPG	IOS	ΔAngle difference	Patient	Arch	Support	Implant
16	0.1419	2.8905	−2.7486	4	Maxilla	6 Implants	16
21	0.4563	2.0836	−1.6273	6	Maxilla	6 Implants	25
31	0.1397	2.0441	−1.9044	7	Mandible	4 Implants	31

Abbreviations: IOS, intraoral optical scanning; SPG, stereophotogrammetry.

The null hypothesis was rejected as SPG performed better than IOS both in terms of 3D (ΔEUC) ($p = .0143$) and angular deviations (ΔANGLE) ($p < .0001$). No effect of the type of arch (maxilla vs. mandible) or number of implants (4 vs. 6) on SPG and IOS accuracy was detected. Previous studies have evaluated the accuracy of various IOSs for complete-arch implant impressions, but a consensus has

TABLE 4 Estimates of fixed effects on ΔEUC (logarithmic scale).

Effect	Estimate	Standard error	*t*-Value	*F*-value	*p*-Value
Intercept	4.28	0.29			
Device (SPG vs. IOS)	−0.42	0.17	−2.45	6.02	.0162
Type of arch (mandible vs. maxilla)	0.31	0.32	0.98	0.96	.3294
Implant number (6 vs. 4)	0.36	0.34	1.06	1.12	.2926

Abbreviations: IOS, intraoral optical scanning; SPG, stereophotogrammetry.

TABLE 5 Estimates of fixed effects on ΔANGLE (logarithmic scale).

Effect	Estimate	Standard error	*t*-Value	*F*-value	*p*-Value
Intercept	−0.55	0.20			
Device (SPG vs. IOS)	−0.67	0.15	−4.48	20.10	<.0001
Type of arch (mandible vs. maxilla)	0.03	0.22	0.12	0.01	.9067
Implant number (6 vs. 4)	0.10	0.23	0.42	0.18	.6755

Abbreviations: IOS, intraoral optical scanning; SPG, stereophotogrammetry.

not been reached on the feasibility of this technique in the daily routine (Amin et al., 2017; Chochlidakis et al., 2020; Pesce et al., 2018; Treesh et al., 2018). Currently, there is no consensus regarding the range of acceptable misfits and the way to correctly measure the misfit clinically (Abduo, 2012; Katsoulis et al., 2017). However, a threshold value of 150 μm was suggested to avoid long-term complications such as loss of retention, screw loosening, fracture of framework, or veneering material (Jemt & Lie, 1995; Mericske-Stern & Worni, 2014; Schwarz, 2000). Moreover, the extreme values in terms of 3D and angular deviations of a single implant in a complete arch supported by 4 and 6 implants were established as 150 and 50 μm in the horizontal and vertical planes and 1° in terms of angulation (Manzella et al., 2016). Moreover, as the implant number increases, the tolerance of the error in the three axes and the angulations decrease (de França et al., 2017). Furthermore, we must consider the manufacturing tolerance of the prosthetic suprastructures that can generate misfits in the form of gaps between 20 and 100 μm (Ortorp et al., 2003). A recent in vitro study investigating the same SPG device reported SPG might be a clinically acceptable alternative to conventional complete-arch implant impressions. However, splinted elastomeric impression method obtained statistically significantly higher overall accuracy, with a trueness difference of 3 μm and a precision difference of 18 μm between the systems (Revilla-León et al., 2023). In the present study, the mean errors associated with the use of SPG were always less than those related to IOS but for the lateral axis (Δ*X*). The greatest difference was found on the longitudinal axis (Δ*Z*), with SPG experiencing 20.9 μm (SD 79.1) and IOS −41.9 μm (SD 127.5). Moreover, the overall 3D deviations in the three axes were significantly in favor of SPG with 87.6 μm (SD 74.2) versus 137.2 μm (SD 115.5) of IOS and far below the accepted threshold value to achieve long-term clinical prognosis of complete-arch implant-supported prostheses. In terms of angle, the mean deviation for each implant position was significant in favor of SPG with 0.38° (SD 0.29) versus 0.79° (SD 0.59) of IOS. The clinical meaning of this 0.40° angular deviation difference has to be further interpreted considering the overall number of implants for each complete arch. Moreover, the extreme differences recorded between the two investigated devices' deviations for each implant position was up to 2.7486° in favor of SPG. Such differences may advise the use of SPG as a more reliable alternative than IOS for complete-arch digital implant impression. Even though a rigid prototype try-in is still recommended before manufacturing definitive screw-retained complete-prostheses, similar outcomes were reported in a recent in vivo study related to two different IOS and SPG systems, whose clinical performance was not analyzed and compared in the same patient (Yan et al., 2022). SPG was more accurate than IOS (range 2.70–92.80 μm, median 17.00 vs. 21.30 to 815.60 μm, and median of 48.95 μm) and not affected by the position or number of implants. The passive fits of the prosthetic frameworks fabricated by SPG, and laboratory scanning were comparable. Another in vivo study analyzed the accuracy of two IOSs and one SPG device in both arches of a single patient. SPG reported the best repeatability in terms of interimplant distance and angular deviation. The type of arch did not affect the SPG accuracy, while the IOSs performed worse in the mandible (Orejas-Perez et al., 2022). In the present study, SPG achieved lower SD in all the linear, 3D and angular deviations than IOS.

The reported IOS means 3D and angular values may negatively affect the overall implant–prosthesis fit, while SPG performed significantly better in terms of 3D and angular deviations; thus, its clinical application for complete-arch digital impression is more advisable and feasible. It has to be considered that the reported deviations are related only to the impression process and therefore are not inclusive of the errors deriving from the other steps necessary to fabricate an implant-supported prosthesis. However, both systems reported extreme deviations far above the clinically accepted

threshold value (IOS 558.1 μm [ΔEUC] and 2.89° [ΔANGLE]; SPG 316.2 μm and 1.92°); therefore, SPG clinical application in a daily routine should be executed with caution, and a rigid prototype try-in is strongly recommended before manufacturing definitive screw-retained complete-arch prostheses. Further clinical investigations are necessary to record accurate data on a larger sample size, especially for the effect of type of arch and number of implants on ΔEUC. Moreover, the impact of the other production steps should be investigated to validate the investigated technologies and the related CAD-CAM workflow for producing screw-retained zirconia-based complete-arch FDPs.

5 | CONCLUSIONS

Within study limitations, SPG performed significantly better than intra-oral scanners with lower 3D and angular deviations and consistent performance. Higher extreme deviations were experienced for IOS. No effect of the type of arch or implant number was detected. SPG can be feasible for complete-arch digital impression. Its clinical application must be executed with caution, and a rigid prototype try-in is recommended before manufacturing definitive screw-retained complete-arch prostheses.

AUTHOR CONTRIBUTIONS

Alessandro Pozzi: Conceptualization; investigation; writing—original draft; methodology; validation; visualization; writing—review and editing; project administration; supervision; resources. **Paolo Carosi:** Conceptualization; investigation; writing—original draft; methodology; validation; visualization; writing—review and editing; project administration; supervision; resources; software; data curation. **German O. Gallucci:** Writing—original draft; writing—review and editing; supervision; conceptualization; methodology. **Katalin Nagy:** Writing—original draft; writing—review and editing; supervision; methodology; conceptualization. **Alessandra Nardi:** Formal analysis; software; data curation; conceptualization; writing—original draft; methodology; writing—review and editing; supervision. **Lorenzo Arcuri:** Conceptualization; investigation; writing—original draft; methodology; writing—review and editing; supervision; data curation; project administration.

ACKNOWLEDGMENTS

MIUR Excellence Department Project awarded to the Department of Mathematics, University of Rome Tor Vergata, Moretti Paglia Dental Lab, Rome, Italy.

CONFLICT OF INTEREST STATEMENT

The authors have stated explicitly that there are no conflicts of interest to disclose in connection with this article.

DATA AVAILABILITY STATEMENT

According to the University Institution regulations on the clinical trials, study data are in the University repository and not publicly available to avoid compromising ethical standards and legal requirements. However, study data may be available on request from the corresponding author in respect of privacy and ethical restrictions.

ETHICS STATEMENT

The study was approved by the Ethical Committee of the University of Rome Tor Vergata protocol number 203/20.

PATIENT CONSENT STATEMENT

All involved participants gave their informed consent prior to study inclusion.

PERMISSION TO REPRODUCE MATERIAL FROM OTHER SOURCES

No permission to reproduce material from other sources was needed.

CLINICAL TRIAL REGISTRATION

University of Rome Tor Vergata Clinical Trial protocol number 203/20 and registered with the identifier ISRCTN12501259.

ORCID

Alessandro Pozzi https://orcid.org/0000-0002-3052-8186
Paolo Carosi https://orcid.org/0000-0002-2442-1091
German O. Gallucci https://orcid.org/0000-0001-6386-594X

REFERENCES

Abduo, J. (2012). Fit of CAD/CAM implant frameworks: A comprehensive review. *Journal of Oral Implantology*, *4*, 758–766. https://doi.org/10.1563/aaid-joi-d-12-00117.1

Abduo, J., Lyons, K., & Swain, M. (2010). Fit of zirconia fixed partial denture: A systematic review. *Journal of Oral Rehabilitation*, *37*(11), 866–876. https://doi.org/10.1111/j.1365-2842.2010.02113.x

Agliardi, E. L., Pozzi, A., Stappert, C. F. J., Benzi, R., Romeo, D., & Gherlone, E. (2012). Immediate fixed rehabilitation of the edentulous maxilla: A prospective clinical and radiological study after 3 years of loading. *Clinical Implant Dentistry and Related Research*, *16*(2), 292–302. https://doi.org/10.1111/j.1708-8208.2012.00482.x

Agliardi, E. L., Pozzi, A., Romeo, D., & Fabbro, M. D. (2023). Clinical outcomes of full-arch immediate fixed prostheses supported by two axial and two tilted implants: A retrospective cohort study with 12–15 years of follow-up. *Clinical Oral Implants Research*, *34*(4), 351–366. https://doi.org/10.1111/clr.14047

Aglietta, M., Siciliano, V. I., Zwahlen, M., Brägger, U., Pjetursson, B. E., Lang, N. P., & Salvi, G. E. (2009). A systematic review of the survival and complication rates of implant supported fixed dental prostheses with cantilever extensions after an observation period of at least 5 years. *Clinical Oral Implants Research*, *20*(5), 441–451. https://doi.org/10.1111/j.1600-0501.2009.01706.x

Agustín-Panadero, R., Peñarrocha-Oltra, D., Gomar-Vercher, S., & Peñarrocha-Diago, M. (2015). Stereophotogrammetry for recording the position of multiple implants: Technical description. *The International Journal of Prosthodontics*, *28*(6), 631–636. https://doi.org/10.11607/ijp.4146

Amin, S., Weber, H. P., Finkelman, M., Rafie, K. E., Kudara, Y., & Papaspyridakos, P. (2017). Digital vs. conventional full-arch implant impressions: A comparative study. *Clinical Oral Implants Research*, *28*(11), 1360–1367. https://doi.org/10.1111/clr.12994

Arcuri, L., Pozzi, A., Lio, F., Rompen, E., Zechner, W., & Nardi, A. (2020). Influence of implant scanbody material, position and operator on

the accuracy of digital impression for complete-arch: A randomized in vitro trial. *Journal of Prosthodontic Research*, *64*(2), 128–136. https://doi.org/10.1016/j.jpor.2019.06.001

Chochlidakis, K., Papaspyridakos, P., Tsigarida, A., Romeo, D., Chen, Y., Natto, Z., & Ercoli, C. (2020). Digital versus conventional full-arch implant impressions: A prospective study on 16 edentulous maxillae. *Journal of Prosthodontics*, *29*(4), 281–286. https://doi.org/10.1111/jopr.13162

de França, D., Morais, M., das Neves, F., Carreiro, A., & Barbosa, G. (2017). Precision fit of screw-retained implant-supported fixed dental prostheses fabricated by CAD/CAM, copy-milling, and conventional methods. *The International Journal of Oral & Maxillofacial Implants*, *32*(3), 507–513. https://doi.org/10.11607/jomi.5023

Flügge, T. V., Att, W., Metzger, M. C., & Nelson, K. (2016). Precision of dental implant digitization using intraoral scanners. *The International Journal of Prosthodontics*, *29*(3), 277–283. https://doi.org/10.11607/ijp.4417

Gómez-Polo, M., Gómez-Polo, C., del Río, J., & Ortega, R. (2018). Stereophotogrammetric impression making for polyoxymethylene, milled immediate partial fixed dental prostheses. *The Journal of Prosthetic Dentistry*, *119*(4), 506–510. https://doi.org/10.1016/j.prosdent.2017.04.029

Huang, R., Liu, Y., Huang, B., Zhang, C., Chen, Z., & Li, Z. (2020). Improved scanning accuracy with newly designed scan bodies: An in vitro study comparing digital versus conventional impression techniques for complete-arch implant rehabilitation. *Clinical Oral Implants Research*, *31*(7), 625–633. https://doi.org/10.1111/clr.13598

Imburgia, M., Logozzo, S., Hauschild, U., Veronesi, G., Mangano, C., & Mangano, F. G. (2017). Accuracy of four intraoral scanners in oral implantology: A comparative in vitro study. *BMC Oral Health*, *17*(1), 92. https://doi.org/10.1186/s12903-017-0383-4

Jemt, T., & Lie, A. (1995). Accuracy of implant-supported prostheses in the edentulous jaw. Analysis of precision of fit between cast gold-alloy frameworks and master casts by means of a three-dimensional photogrammetric technique. *Clinical Oral Implants Research*, *6*(3), 172–180. https://doi.org/10.1034/j.1600-0501.1995.060306.x

Johansson, A., Omar, R., & Carlsson, G. E. (2011). Bruxism and prosthetic treatment: A critical review. *Journal of Prosthodontic Research*, *55*(3), 127–136. https://doi.org/10.1016/j.jpor.2011.02.004

Kan, J. Y. K., Rungcharassaeng, K., Bohsali, K., Goodacre, C. J., & Lang, B. R. (1999). Clinical methods for evaluating implant framework fit. *The Journal of Prosthetic Dentistry*, *81*(1), 7–13. https://doi.org/10.1016/s0022-3913(99)70229-5

Katsoulis, J., Takeichi, T., Gaviria, A. S., Peter, L., & Katsoulis, K. (2017). Misfit of implant prostheses and its impact on clinical outcomes. Definition, assessment and a systematic review of the literature. *European Journal of Oral Implantology*, *10*(Suppl 1), 121–138.

Kihara, H., Hatakeyama, W., Komine, F., Takafuji, K., Takahashi, T., Yokota, J., Oriso, K., & Kondo, H. (2019). Accuracy and practicality of intraoral scanner in dentistry: A literature review. *Journal of Prosthodontic Research*, *64*(2), 109–113. https://doi.org/10.1016/j.jpor.2019.07.010

Lie, A., & Jemt, T. (1994). Photogrammetric measurements of implant positions. Description of a technique to determine the fit between implants and superstructures: Photogrammetric measurements of implant positions. *Clinical Oral Implants Research*, *5*(1), 30–36. https://doi.org/10.1034/j.1600-0501.1994.050104.x

Ma, B., Yue, X., Sun, Y., Peng, L., & Geng, W. (2021). Accuracy of photogrammetry, intraoral scanning, and conventional impression techniques for complete-arch implant rehabilitation: An in vitro comparative study. *BMC Oral Health*, *21*(1), 636. https://doi.org/10.1186/s12903-021-02005-0

Manzella, C., Bignardi, C., Burello, V., Carossa, S., & Schierano, G. (2016). Method to improve passive fit of frameworks on implant-supported prostheses: An in vitro study. *The Journal of Prosthetic Dentistry*, *116*(1), 52–58. https://doi.org/10.1016/j.prosdent.2016.01.006

Mericske-Stern, R., & Worni, A. (2014). Optimal number of oral implants for fixed reconstructions: A review of the literature. *European Journal of Oral Implantology*, *7*(Suppl 2), S133–S153.

Mizumoto, R. M., Yilmaz, B., McGlumphy, E. A., Seidt, J., & Johnston, W. M. (2020). Accuracy of different digital scanning techniques and scan bodies for complete-arch implant-supported prostheses. *The Journal of Prosthetic Dentistry*, *123*(1), 96–104. https://doi.org/10.1016/j.prosdent.2019.01.003

Orejas-Perez, J., Gimenez-Gonzalez, B., Ortiz-Collado, I., Thuissard, I. J., & Santamaria-Laorden, A. (2022). In vivo complete-arch implant digital impressions: Comparison of the precision of three optical impression systems. *International Journal of Environmental Research and Public Health*, *19*(7), 4300. https://doi.org/10.3390/ijerph19074300

Ortorp, A., Jemt, T., Bäck, T., & Jälevik, T. (2003). Comparisons of precision of fit between cast and CNC-milled titanium implant frameworks for the edentulous mandible. *The International Journal of Prosthodontics*, *16*(2), 194–200.

Peñarrocha-Diago, M., Balaguer-Martí, J. C., Peñarrocha-Oltra, D., Balaguer-Martínez, J. F., Peñarrocha-Diago, M., & Agustín-Panadero, R. (2017). A combined digital and stereophotogrammetric technique for rehabilitation with immediate loading of complete-arch, implant-supported prostheses: A randomized controlled pilot clinical trial. *The Journal of Prosthetic Dentistry*, *118*(5), 596–603. https://doi.org/10.1016/j.prosdent.2016.12.015

Peroz, S., Spies, B. C., Adali, U., Beuer, F., & Wesemann, C. (2021). Measured accuracy of intraoral scanners is highly dependent on methodical factors. *Journal of Prosthodontic Research*, *66*(2), 318–325. https://doi.org/10.2186/jpr.jpr_d_21_00023

Pesce, P., Pera, F., Setti, P., & Menini, M. (2018). Precision and accuracy of a digital impression scanner in full-arch implant rehabilitation. *The International Journal of Prosthodontics*, *31*(2), 171–175. https://doi.org/10.11607/ijp.5535

Pozzi, A., Arcuri, L., Block, M. S., & Moy, P. K. (2020). Digital assisted soft tissue sculpturing (DASS) technique for immediate loading pink free complete arch implant prosthesis. *Journal of Prosthodontic Research*, *65*(1), 119–124. https://doi.org/10.2186/jpr.jpor_2019_386

Pozzi, A., Arcuri, L., Carosi, P., Nardi, A., & Kan, J. (2021). Clinical and radiological outcomes of novel digital workflow and dynamic navigation for single-implant immediate loading in aesthetic zone: 1-year prospective case series. *Clinical Oral Implants Research*, *32*(12), 1397–1410. https://doi.org/10.1111/clr.13839

Pozzi, A., Arcuri, L., Fabbri, G., Singer, G., & Londono, J. (2021). Long-term survival and success of zirconia screw-retained implant-supported prostheses for up to 12 years: A retrospective multicenter study. *The Journal of Prosthetic Dentistry.*, *129*, 96–108. https://doi.org/10.1016/j.prosdent.2021.04.026

Pozzi, A., Arcuri, L., Lio, F., Papa, A., Nardi, A., & Londono, J. (2022). Accuracy of complete-arch digital implant impression with or without scanbody splinting: An in vitro study. *Journal of Dentistry*, *119*, 104072. https://doi.org/10.1016/j.jdent.2022.104072

Pozzi, A., Hansson, L., Carosi, P., & Arcuri, L. (2020). Dynamic navigation guided surgery and prosthetics for immediate loading of complete-arch restoration. *Journal of Esthetic and Restorative Dentistry: Official Publication of the American Academy of Esthetic Dentistry*, *33*(1), 224–236. https://doi.org/10.1111/jerd.12710

Pozzi, A., Tallarico, M., & Barlattani, A. (2013). Monolithic lithium disilicate full-contour crowns bonded on CAD/CAM zirconia complete-arch implant bridges with 3 to 5 years of follow-up. *The Journal of Oral Implantology*, *41*(4), 450–458. https://doi.org/10.1563/aaid-joi-d-13-00133

Pozzi, A., Tallarico, M., Mangani, F., & Barlattani, A. (2013). Different implant impression techniques for edentulous patients treated with CAD/CAM complete-arch prostheses: A randomised controlled trial reporting data at 3 year post-loading. *European Journal of Oral Implantology*, *6*(4), 325–340.

Pradíes, G., Ferreiroa, A., Özcan, M., Giménez, B., & Martínez-Rus, F. (2014). Using stereophotogrammetric technology for obtaining intraoral digital impressions of implants. *The Journal of the American Dental Association*, *145*(4), 338–344. https://doi.org/10.14219/jada.2013.45

Revilla-León, M., Att, W., Özcan, M., & Rubenstein, J. (2021). Comparison of conventional, photogrammetry, and intraoral scanning accuracy of complete-arch implant impression procedures evaluated with a coordinate measuring machine. *The Journal of Prosthetic Dentistry*, *125*(3), 470–478. https://doi.org/10.1016/j.prosdent.2020.03.005

Revilla-León, M., Rubenstein, J., Methani, M. M., Piedra-Cascón, W., Özcan, M., & Att, W. (2023). Trueness and precision of complete-arch photogrammetry implant scanning assessed with a coordinate-measuring machine. *The Journal of Prosthetic Dentistry*, *129*(1), 160–165. https://doi.org/10.1016/j.prosdent.2021.05.019

Rungruanganunt, P., Taylor, T., Eckert, S. E., & Karl, M. (2013). The effect of static load on dental implant survival: A systematic review. *The International Journal of Oral & Maxillofacial Implants*, *28*(5), 1218–1225. https://doi.org/10.11607/jomi.2888

Rutkūnas, V., Gečiauskaitė, A., Jegelevičius, D., & Vaitiekūnas, M. (2017). Accuracy of digital implant impressions with intraoral scanners. A systematic review. *European Journal of Oral Implantology*, *10*(Suppl 1), 101–120.

Sanda, M., Miyoshi, K., & Baba, K. (2021). Trueness and precision of digital implant impressions by intraoral scanners: A literature review. *International Journal of Implant Dentistry*, *7*(1), 97. https://doi.org/10.1186/s40729-021-00352-9

Schwarz, M. S. (2000). Mechanical complications of dental implants. *Clinical Oral Implants Research*, *11*(S1), 156–158. https://doi.org/10.1034/j.1600-0501.2000.011s1156.x

Treesh, J. C., Liacouras, P. C., Taft, R. M., Brooks, D. I., Raiciulescu, S., Ellert, D. O., Grant, G. T., & Ye, L. (2018). Complete-arch accuracy of intraoral scanners. *The Journal of Prosthetic Dentistry*, *120*(3), 382–388. https://doi.org/10.1016/j.prosdent.2018.01.005

von Elm, E., Altman, D. G., Egger, M., Pocock, S. J., Gøtzsche, P. C., Vandenbroucke, J. P., & STROBE Initiative. (2014). The Strengthening the Reporting of Observational Studies in Epidemiology (STROBE) Statement: guidelines for reporting observational studies. *International journal of surgery*, *12*(12), 1495–1499. https://doi.org/10.1016/j.ijsu.2014.07.013

Yan, Y., Lin, X., Yue, X., & Geng, W. (2022). Accuracy of 2 direct digital scanning techniques—Intraoral scanning and stereophotogrammetry—For complete arch implant-supported fixed prostheses: A prospective study. *The Journal of Prosthetic Dentistry*, S0022-3913(22)00216-5. https://doi.org/10.1016/j.prosdent.2022.03.033

SUPPORTING INFORMATION

Additional supporting information can be found online in the Supporting Information section at the end of this article.

How to cite this article: Pozzi, A., Carosi, P., Gallucci, G. O., Nagy, K., Nardi, A., & Arcuri, L. (2023). Accuracy of complete-arch digital implant impression with intraoral optical scanning and stereophotogrammetry: An in vivo prospective comparative study. *Clinical Oral Implants Research*, *00*, 1–12. https://doi.org/10.1111/clr.14141